U-Pb Zircon Geochronology and Nd Isotopic Signatures of the Pre-Mesozoic Metamorphic Basement of the Eastern Peruvian Andes: Growth and Provenance of a Late Neoproterozoic to Carboniferous Accretionary Orogen on the Northwest Margin of Gondwana

A. Cardona, U. G. Cordani,[1] *J. Ruiz,*[2] *V. A. Valencia,*[2] *R. Armstrong,*[3] *D. Chew,*[4] *A. Nutman,*[5] *and A. W. Sanchez*[6]

Smithsonian Tropical Research Institute, Balboa, Ancón, Panama
(e-mail: cardonaa@si.edu)

ABSTRACT

This study integrates U-Pb zircon geochronology (from LAM-ICP-MS, SHRIMP, and TIMS) with Nd isotopic data from orthogneisses and metasedimentary rocks of the pre-Mesozoic basement of the eastern Peruvian Andes to provide new information on the tectonic evolution and Neoproterozoic-Paleozoic paleogeography of this segment of the proto-Andean margin. A high-grade orthogneiss unit yields U-Pb zircon protolith crystallization ages of ~613 Ma. It was metamorphosed and intruded by an Early Ordovician granitoid. Subsequently, two different volcano-sedimentary sequences were laid down and metamorphosed, probably as a consequence of terrane accretion. The older sequence was deposited and metamorphosed between 450 and 420 Ma, and the younger one was deposited after 320 Ma and metamorphosed at 310 Ma. U-Pb detrital zircon age patterns from the two sequences are within the age intervals 315–480, 480–860, 960–1400, and >1400 Ma. These data strongly suggest geological and spatial links between the different units, implying the existence of active magmatism contemporaneous with the reworking of previously formed orogenic complexes. Mesoproterozoic and older ages suggest that the detrital sources are on the western margin of Gondwana, near the Amazonian Craton and/or other Grenvillian-type domains, such as those found within the Andean belt. Neoproterozoic to Ordovician zircons suggest that this crustal segment was formed on an active margin along the western side of the Amazonian Craton. Whole-rock Nd isotope data from metasedimentary rocks of the two younger units yield $\varepsilon_{Nd\ (450\ Ma,\ 310\ Ma)}$ values between −6.3 and −13.2 and Sm-Nd T_{DM} model ages between 1.6 and 2.1 Ga. The comparison of the Nd isotope record with the U-Pb detrital zircon data suggests that recycling of older crust was an important factor in the growth of the central Peruvian segment of the proto-Andean margin during the Proterozoic and the Early Paleozoic. Different tectonic and paleogeographic models are discussed in light of the new data presented here.

Online enhancements: appendix tables.

Introduction

The Neoproterozoic to Late Paleozoic tectonic evolution of the proto-Andean margin has been included within the large-scale Terra Australis orogen (Cawood 2005), a major tectonic belt that extends more than 18,000 km along the Pacific margin of Gondwana, from South America to Australia. The growth of this orogen is related to continuous ocean convergence following breakup of Rodinia and the formation of the paleo-Pacific and Iapetus oceans, and culminates with the assembly of Pangaea and the Gondwanide-Alleghenian orogenic event.

Despite considerable advances in the understanding of several elements of this margin, the timing and episodes of arc formation and oceanic plate convergence versus terrane accretion or dispersion are issues that are not fully resolved. The tectonic

Manuscript received June 25, 2008; accepted January 20, 2009.

[1] Instituto de Geociências, Universidade de São Paulo, São Paulo, Brazil CEP 05508-080.

[2] Department of Geosciences, University of Arizona, Tucson, Arizona 85721, U.S.A.

[3] Research School of Earth Sciences, Australian National University, Building 61, Mills Road, Acton, Australian Capital Territory 0200, Australia.

[4] Department of Geology, Trinity College, Dublin 2, Ireland.

[5] Institute of Geology, Chinese Academy of Geological Sciences, 26 Baiwanzhuang Road, Beijing 100037, China.

[6] Instituto Geológico Minero y Metalúrgico, Avenida Canada 1470, San Borja, Lima 41, Peru.

[The Journal of Geology, 2009, volume 117, p. 285–305] 0022-1376/2009/11703-0004$15.00. DOI: 10.1086/597472

evolution of the proto-Andean margin has implications for paleogeographical reconstructions, regional correlation of orogenic phases, and the evolution of ancient margins in general (Pankhurst and Rapela 1998; Keppie and Ramos 1999; Ramos 1999, 2004; Lucassen and Franz 2005).

Along the eastern Peruvian Andes, between 6°S and 12°S a major pre-Mesozoic metamorphic and magmatic province crops out (fig. 1). This segment of the proto-Andean margin has been the focus of recent research (Cardona et al. 2006, 2007; Chew et al. 2007*b*; Ramos 2008*a*). It has major implications for the Neoproterozoic paleogeography of the western Amazonian Craton during Rodinia breakup (Chew et al. 2008), the formation and drift of para-autochthonous Gondwanide terranes, and the Late Paleozoic transition from Laurentia-Gondwana tectonic interactions in the northern Andes

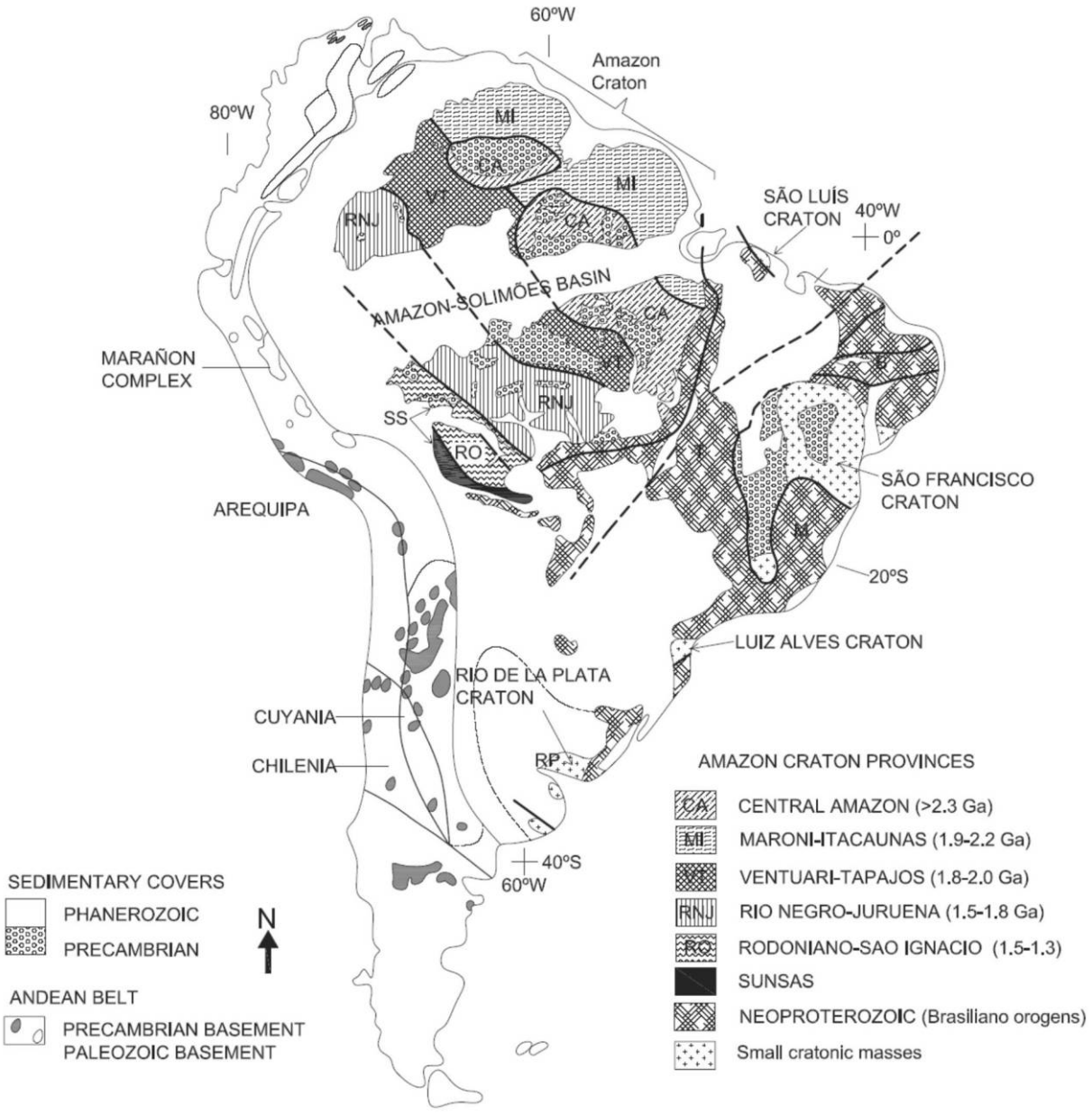

Figure 1. Geochronological provinces of the Amazonian Craton and pre-Mesozoic Andean inliers, including the Marañon Complex (modified from Cordani et al. 2000). Published Paleozoic and Precambrian U-Pb crystallization ages from Peru are after Dalmayrac et al. (1988); Wasteneys et al. (1995); Loewy et al. (2004); Chew et al. (2007*b*).

and the major Gondwanide orogenic cycle to the south (Bahlburg 1993; Ramos and Aleman 2000; Cawood 2005; Murphy et al. 2004; Ramos 2008*a*).

Detrital U-Pb zircon geochronology and Sm-Nd whole-rock isotopic analyses from sedimentary rocks are valuable tools for tectonic, stratigraphic and provenance studies (see McLennan et al. 1993; Dickinson and Gehrels 2001; Fedo et al. 2003). When integrated with U-Pb zircon magmatic and metamorphic crystallization ages, they provide a robust tectonostratigraphic framework to trace the evolving nature of an orogen.

In this article, we integrate U-Pb laser ablation–multicollector–inductively coupled plasma–mass spectrometry (LAM-ICP-MS) and SHRIMP measurements on detrital zircons, whole-rock Sm-Nd analyses from metasedimentary rocks, and U-Pb SHRIMP and TIMS zircon crystallization ages from gneisses and granitoids from the pre-Triassic metamorphic basement of the eastern Peruvian Andes at ~10°S (fig. 2). These data are used to constrain the sedimentary, magmatic, and metamorphic evolution of this segment of the proto-Andean margin.

Geological Setting of the Peruvian Andes. The central Peruvian Andes between 6°S and 14°S (fig. 2) correspond to one of the present-day flat-slab subduction segments below the Andean chain. Its geological framework includes a prominent Late Mesozoic to Cenozoic volcano-sedimentary and plutonic belt in the Western Cordillera and adjacent coastal regions (Pitcher and Cobbing 1985; Benavides-Cáceres 1999). Controversy remains about the nature of the basement within this region. Some authors favor the absence of continental basement (Polliand et al. 2005), while others suggest that the available geological and geophysical evidence points to a sialic substrate (Ramos 2008*a*).

Sedimentary, plutonic, and metamorphic units attributed to Paleozoic or older pre-Andean cycles are confined to the Eastern Cordillera (fig. 2). The sedimentary units include fossiliferous Ordovician, Mississippian, and Late Permian sequences (Dalmayrac et al. 1988; Zapata et al. 2005), whereas magmatic rocks range in age between the Ordovician to Early Triassic (Macfarlane et al. 1999; Miskovic et al. 2005; Cardona 2006; Chew et al. 2007*b*). An extensive but discontinuous series of metamorphic units is also exposed in the core of the Eastern Cordillera. Commonly referred to as the Marañon Complex (Wilson and Reyes 1964), this belt was initially considered pre-Ordovician (probably Neoproterozoic) based on local exposures of undeformed Ordovician rocks and a Neoproterozoic U-Pb zircon lower intercept age from a migmatitic paragneiss (Wilson and Reyes 1964; Dalmayrac et al. 1988). However, the results presented here, combined with recently published geological constraints from other segments of the Eastern Cordillera (Chew et al. 2007*b*), demonstrate the existence of a more complex Paleozoic tectonic evolution.

Other Proterozoic, Paleozoic, and Triassic plutonic and metamorphic domains, such as the Illescas Massif and the Arequipa-Antofalla terrane, are exposed in the coastal region of Peru (fig. 2; Wasteneys et al. 1995; Loewy et al. 2004; Chew et al. 2007*a*; Cardona et al. 2008). Late Mesoproterozoic granulite-facies rocks, which are probably part of the Amazonian Craton, have also been reported from the Picharí river in the Amazon region of Peru (fig. 2; Dalmayrac et al. 1988).

The Marañon Complex. The term "Marañon Complex" has been commonly used in the geological literature to include all metamorphic basement rocks of the Eastern Cordillera (Wilson and Reyes 1964; Dalmayrac et al. 1988). This composite unit discontinuously extends for more than 500 km between 6°S and 12°S (fig. 2) and includes various low- to middle-grade metamorphic belts of volcano-sedimentary origin. Higher-grade domains are restricted in extent. Stratigraphic relations include local unconformities with overlying Ordovician, Carboniferous, or Permian sediments and intrusive contacts with Late Paleozoic granitoids (Wilson and Reyes 1964; Dalmayrac et al. 1988; Cardona 2006; Chew et al. 2007*b*).

Previous temporal constraints for the geologic evolution of this metamorphic basement were based on regional extrapolation of local unconformities with the Early Ordovician fossiliferous sediments, and the previously mentioned Neoproterozoic U-Pb zircon lower intercept age from a migmatitic paragneiss. This loosely constrained ca. 630–610-Ma age was considered as evidence for a Neoproterozoic orogeny on this segment of the proto-Andean margin (Dalmayrac et al. 1988). However, as discussed here and also presented by Cardona et al. (2007) and Chew et al. (2007*a*), this metamorphic basement include several units with a more complicated Neoproterozoic to Late Paleozoic geological record.

Local Geology and Sampling Constraints. The Marañon Complex was sampled close to the towns of Huánuco and La Unión at ~10°S, (fig. 3). This region is where the unconformable relationships with fossiliferous Paleozoic rocks as well as the 610–630-Ma U-Pb zircon age of Dalmayrac et al. (1988) were originally reported. Zircons from 10 samples of metasedimentary and metaigneous rocks were selected for U-Pb analysis by different

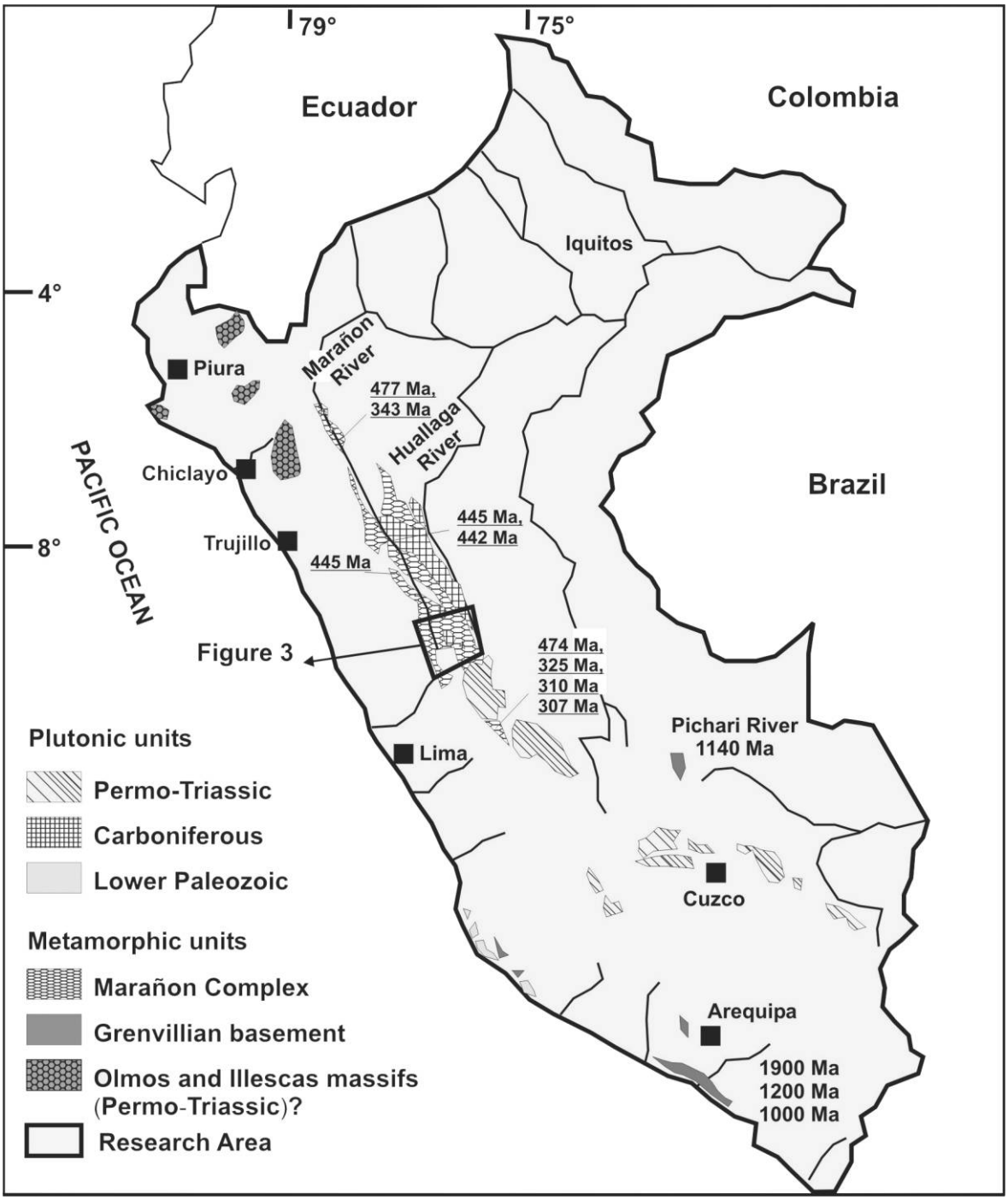

Figure 2. Pre-Mesozoic plutonic and metamorphic rocks of the Peruvian Andes.

techniques (fig. 3), while 18 metasedimentary whole-rock samples were analyzed for Sm-Nd isotopes (fig. 3).

Based on lithostratigraphic correlation and local relationships with Paleozoic sedimentary rocks, we divide the Marañon Complex into four main units (fig. 3). (1) A small inlier of amphibolite-facies gneisses yields peak metamorphic temperatures of 590°–615°C (Cardona et al. 2007) and is intruded by a mylonitized granitoid. This inlier is enclosed within unit (2), a belt of micaceous schists with sporadic intercalations of metabasite and calc-sil-

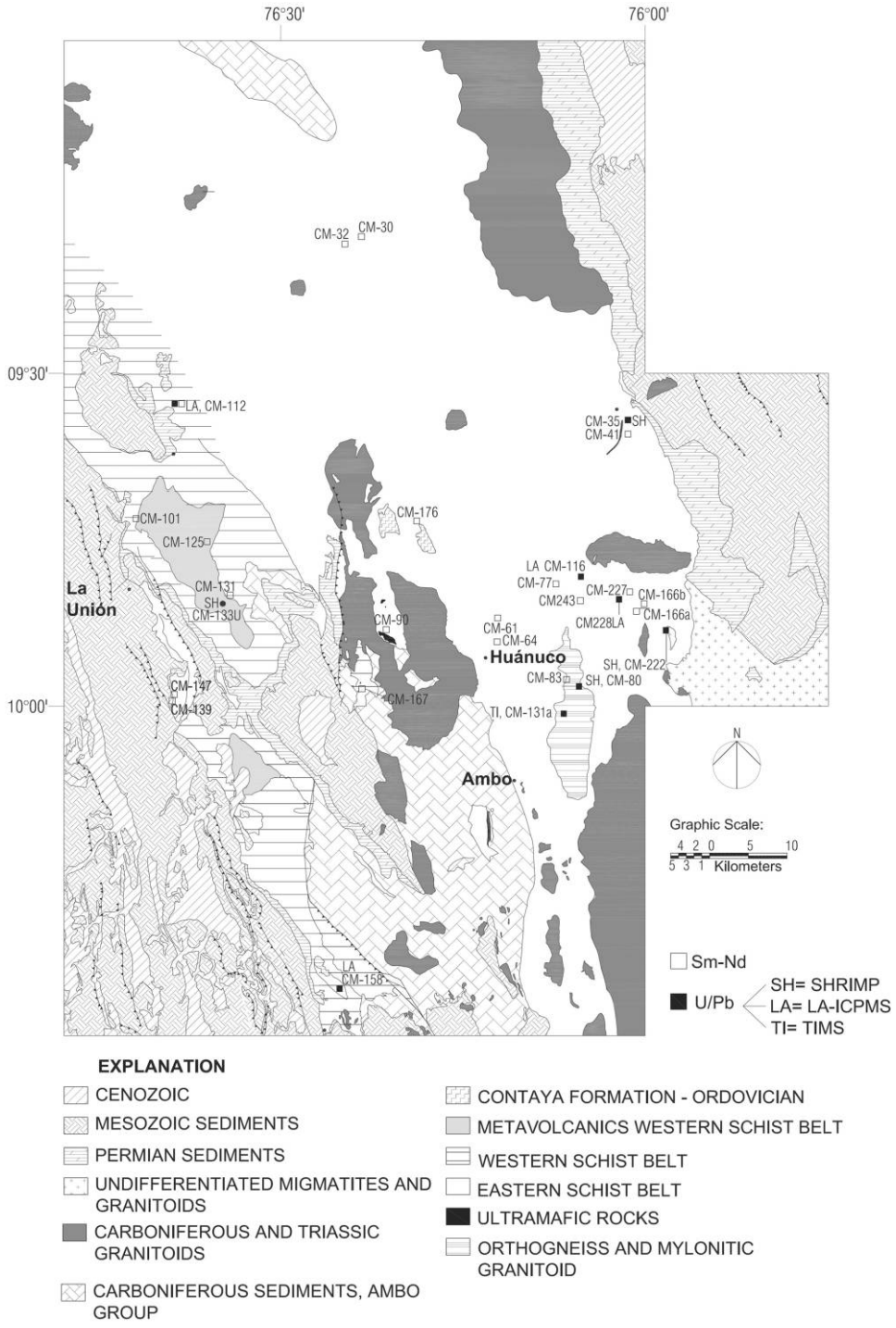

Figure 3. Geological map of the Marañon Complex in the Huánuco–La Unión regions (modified from Cobbing and Sanchez 1996*a*, 1996*b*; De la Cruz and Valencia 1996; Quispesivana 1996; Martinez et al. 1998).

icate rocks, defined here as the Eastern Schist Belt (ESB). Metamorphic grade varies from lower greenschist to amphibolite facies, with calculated *PT* conditions ranging from 3–5 kbar and 350°–450°C to 7–10 kbar and 540°–660°C. These peak metamorphic assemblages are in turn affected by a lower-grade greenschist-facies crenulation cleavage (Cardona et al. 2007). Mafic and ultramafic rocks

crop out as discontinuous lenses along the eastern margin of this belt (Grandin and Navarro 1979). Fossiliferous Carboniferous sedimentary rocks unconformably overlie the eastern schists (Dalmaryac et al. 1988). (3) A series of isolated migmatite bodies is spatially linked to some undeformed granitoids that outcrop within the ESB. (4) A western belt of mica schists, referred to here as the Western Schist Belt (WSB), is characterized by significant intercalations of metabasite. Metamorphic grade is mainly in the greenschist facies, with peak metamorphic conditions of 3–4 kbar and 350°–400°C (Cardona et al. 2007). This belt is covered by Permian sedimentary rocks. Minor remnants of ultramafic rocks with associated phyllites and slates that crop out on the eastern margin of the western schists are in thrust contact with Carboniferous sediments of the Ambo Group (Grandin and Navarro 1979).

Triassic granitoids clearly intrude both eastern and western schist belts (Cardona 2006). The western belt is separated from the eastern belt by undeformed Carboniferous sedimentary rocks of the Ambo Group and remnants of weakly deformed fossiliferous Ordovician rocks (Dalmayrac et al. 1988). Geochemical constraints from the metavolcanic units combined with Ar-Ar and Rb-Sr geochronology suggest that the protoliths of the two belts were deposited in an arc-related setting and that they experienced major metamorphic events during the Silurian (eastern schists, ~420 Ma) and Late Carboniferous (western schists, 300–310 Ma; Cardona 2006; Cardona et al. 2007). A garnetiferous gneiss associated with a banded migmatite body in the ESB sampled at the the same locality where Dalmayrac et al. (1988) report their Neoproterozoic metamorphic age yielded a Sm-Nd garnet-whole-rock isochron of ca. 295 Ma (Cardona 2006).

Analytical Techniques. Zircon separates and whole-rock powders were prepared following standard procedures at the laboratories of the Geochronological Research Center of the University of São Paulo (CPGeo-USP) and also following Basei et al. (1995) and Sato et al. (1995). All radiometric data used the decay constants listed in Steiger and Jäger (1977). U-Pb concordia ages and relative probability diagrams were calculated using the program Isoplot/Ex 3.0 of Ludwig (2003). Tables A1 and A2, available in the online edition or from the *Journal of Geology* office, show the U-Pb analytical results and the Sm-Nd isotopic data, respectively.

U-Pb LAM-ICP-MS Analyses

U-Pb analyses were undertaken at the University of Arizona LaserChron laboratory following the procedures described by Gehrels et al. (2006). Unknowns and standard zircons were mounted in the central portion of the mount area to reduce possible fractionation effects. The grains analyzed were selected randomly from the zircon population on the sample mount. In detrital samples, grain cores were analyzed to avoid possible thin metamorphic overgrowths. Zircon crystals were analyzed with a VG isoprobe multicollector ICP–MS equipped with nine Faraday collectors, an axial Daly collector, and four ion-counting channels. The isoprobe is equipped with an ArF excimer laser ablation system, which has an emission wavelength of 193 nm. The collector configuration allows measurement of ^{204}Pb in the ion-counting channel while ^{206}Pb, ^{207}Pb, ^{208}Pb, ^{232}Th, and ^{238}U are simultaneously measured with Faraday detectors. All analyses were conducted in static mode with a laser beam diameter of 35–50 μ, operated with an output energy of ~32 mJ (at 23 kV) and a pulse rate of 8 Hz. Each analysis consisted of one 20-s integration on peaks with no laser firing and 20 1-s integrations on peaks with the laser firing. Hg contribution to the ^{204}Pb mass position was removed by subtracting on-peak background values. Interelement fractionation was monitored by analyzing an in-house zircon standard, which has a concordant TIMS age of 563.5 ± 3.2 Ma (2σ; Gehrels et al. 2008). This standard was analyzed once for every five unknowns in detrital grains. U and Th concentrations were monitored by analyzing a standard (NIST 610 Glass) with ~500 ppm Th and U. The Pb isotopic ratios were corrected for common Pb, using the measured ^{204}Pb, assuming an initial Pb composition according to Stacey and Kramers (1975).

The uncertainties on the age of the standard, the calibration correction from the standard, the composition of the common Pb, and the decay constant uncertainty are grouped together and are known as the systematic error. For the zircon analyses in this study, the systematic errors range between ~1.0% and 1.4% for the ^{206}Pb/^{238}U ratio and ~0.8% and 1.1% for the ^{207}Pb/^{206}Pb ratio.

U-Pb SHRIMP Analyses

U-Pb determinations on single zircon grains were carried out using the SHRIMP I instrument at the Australian National University. Cathodoluminescence (CL) images were obtained to select zircon domains for each analysis. Because of effects such as the differential yield of metal and oxide species between elements during sputtering, interelement ratios were calibrated with a standard whose isotopic ratios are known by isotope dilution thermal

ionization mass spectrometry (ID-TIMS). Details of the analytical procedures, including calibration methods, were presented by Williams (1998) and Stern (1998). $^{206}Pb/^{238}U$ ratios have an analytical uncertainty of typically 1.5%–2.0% from calibration of the measurements using standard zircons. U abundance was calibrated with fragments of the single crystal SL13 zircon standard (238 ppm U). All errors also take into account nonlinear fluctuations in ion counting rates beyond that expected from counting statistics (Stern 1998).

U-Pb ID-TIMS. Analyses were undertaken at the CPGeo-USP, following Basei et al. (1995). Zircons were mechanically abraded with pyrite for 15 min in a steel capsule, leached with hot HNO_3, rinsed with deionized water, and cleaned in an ultrasonic bath. Isotopic dilution analyses followed standard procedures and employed a mixed Pb-U spike (after Krogh 1973, with minor modification by Basei et al. 1995). The CPGeo uses a VG 354 TIMS with five Faraday cup collectors and a Daly detector.

Sm-Nd Isotopes. Sm-Nd whole-rock analyses were also undertaken at the CPGeo-USP using a Finnegan 262 multicollector mass spectrometer and following the procedures described by Sato et al. (1995). $^{143}Nd/^{144}Nd$ ratios have an analytical uncertainty of 0.014% (2σ). Analytical uncertainty on the $^{147}Sm/^{144}Nd$ ratio is estimated at 0.5%. The La Jolla and BCR-1 standards respectively yielded $^{143}Nd/^{144}Nd$ ratios of 0.511849 ± 0.000025 (1σ) and 0.512662 ± 0.000027 (1σ). Sm-Nd depleted mantle model ages (T_{DM}) were calculated following De Paolo et al. (1991).

U-Pb Geochronological Results

Analytical results are listed in table A1 and sample locations are included on fig. 3. Analyses of detrital zircons with LAM-ICP-MS followed a quantitative approach, and zircons were randomly selected (Gehrels et al. 2006). In order to review metamorphic overgrowths, we obtained CL images of the zircons before the SHRIMP analysis. For zircons with ages >1.0 Ga, $^{207}Pb/^{206}Pb$ ages were preferred, whereas for the younger grains, $^{206}Pb/^{238}U$ ages were preferred. Analyses with discordant values >10% were discarded.

Orthogneiss and Mylonitic Granitoid. This composite unit is part of a high-grade metamorphic inlier within the ESB. It crops out in the high mountains between the towns of Ambo and Huánuco (fig. 3). The granitoid intrudes gneissic rocks, whereas its relationship with the ESB is probably tectonic. Both lithologies were subsequently affected by greenschist-facies mylonitic fabric that is presumably correlative with the foliation in the adjacent ESB.

Zircons from sample CM-80 (9°56′32″S, 76°4′19″W) of the gneissic unit were analyzed by the U-Pb SHRIMP method. This rock contains muscovite and biotite, with strong banding and a mylonitic fabric, and relict magmatic zoned plagioclase porphyroclasts. Estimated metamorphic peak temperatures for the gneissic unit are ~615°C (Cardona et al. 2007). Crystals are euhedral and prismatic. Cathodoluminescence images display variable internal structures of the crystals, including fully oscillatory and homogenous crystals, or homogenous rims surrounding oscillatory cores. Some of the zircons are slightly metamict. A total of 16 analyses were undertaken and yielded concordant ages (fig. 4*A*). Eight homogenous rims, including two spots with a single crystal, yield an age of 484 ± 12 Ma (MSWD = 0.81) with Th/U ratios lower than 0.1 and are interpreted as metamorphic zircon "overgrowths" (Vabra et al. 1999). Six prismatic crystals with oscillatory cores present a $^{206}Pb/^{238}U$ mean age of 613 ± 35 Ma (MSWD = 0.51), which is related to the magmatic protolith, whereas another grain, with a lower Th/U ratio and an age of ca. 990 Ma, is interpreted as a premagmatic xenocryst.

The mylonitized granitoid CM-131A (9°58′41″S, 76°6′20″W; fig. 4*B*) exhibits a strong fabric defined by small muscovite crystals, with associated recrystallized quartz bands that suggest deformational temperatures lower than 400°C (cf. Passchier and Trouw 1996). Five multigrain zircon populations were selected for U-Pb TIMS analysis. Three of the analyzed fractions are strongly concordant, with a $^{206}Pb/^{238}U$ age of 468 ± 5 Ma (MSWD = 0.29) that we interpret as the magmatic crystallization age, whereas the other two fractions are discordant. They present older $^{206}Pb/^{238}U$ ages of >478 Ma, which point to the presence of an older inherited component.

ESB. Detrital zircons from two schist samples collected near the town of Huánuco (fig. 3) were analyzed by the U-Pb LAM-ICP-MS. Sample CM-116 (9°47′7″S, 76°4′19″W) is a greenschist-facies calc-silicate schist, and sample CM-228 (9°49′16″S, 76°1′19″W) is a garnet-mica schist that has yielded *PT* conditions of 600°C and 7 kbar (Cardona et al. 2007).

In general, the zircon crystals are prismatic to rounded, with U/Th ratios <12 that can be related to a former magmatic origin (Rubatto 2002). The 104 dated zircon grains from sample CM-116 yield predominantly concordant ages, with a prominent $^{207}Pb/^{206}Pb$ age population between 960 and 1400

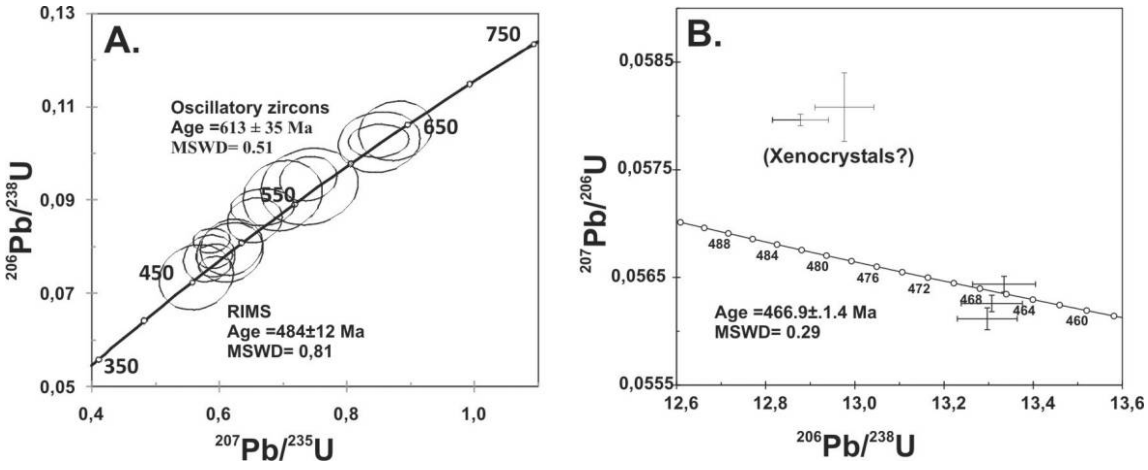

Figure 4. U-Pb concordia diagrams from samples CM-80 (*A*) and CM-131A (*B*).

Ma (n = 86), with 66 of these grains concordant in the 1120–1280-Ma age range (fig. 5*A*). A smaller group of six analyses ranges between 1800 and 1900 Ma, whereas two groups of four grains each yield ages of 800 and 1480 Ma.

Zircons from sample CM-228 are also concordant, with the youngest and oldest ages of 465 ± 6 Ma ($^{206}Pb/^{238}U$) and 2714 ± 16 Ma ($^{207}Pb/^{206}Pb$), respectively (fig. 5*B*). The dominant zircon population ranges between 460 and 860 Ma (n = 71), with most grains yielding ages younger than 620 Ma. Twenty-one grains with Early Neoproterozoic to Mesoproterozoic ages (960–1240 Ma) were also obtained. Two grains have $^{207}Pb/^{206}Pb$ ages of 1365 ± 20 and 1929 ± 27 Ma, while two additional grains are concordant with $^{207}Pb/^{206}Pb$ ages of 2150 ± 26 and 2532 ± 17 Ma. Along with some discordant old grains, this shows the presence of a Paleoproterozoic and Archean detrital component.

ESB Migmatites. Two migmatite bodies spatially associated with the eastern schists were sampled (fig. 3). An apparent metamorphic break is observed between the schists and the migmatites, with the lower-grade greenschist facies changing abruptly to a banded and nebulitic migmatite. Concordant and discordant granite injections crosscut the schists.

Eighteen zircons from the banded migmatite CM-35 (9°34′17″S, 76°0′54″W) that transitionally grade to a micaceous granite and a series of pegmatites were dated by SHRIMP. This sample comes from the same area where Dalmayrac et al. (1988) reported a Neoproterozoic U-Pb zircon lower intercept age from a garnetiferous paragneiss. The grains are prismatic to weakly rounded, with CL images characterized by cores with oscillatory zoning and homogenous rims. The rims have Th/U ratios <1 and yield a well-defined $^{206}Pb/^{238}U$ age of 325 ± 8 Ma (fig. 6*A*). Oscillatory zoned cores yield ages between 400 and 650 Ma.

Zircons from migmatite CM-222 (9°51′50″S, 75°58′32″W) exhibiting nebulitic structure were also analyzed by SHRIMP. Two main zircon populations were observed, a prismatic equidimensional population and a fragmented, ovoid population. Internal structures seen in CL images include oscillatory and homogenous domains. Twleve zircons were analyzed and revealed highly variable ages (fig. 6*B*). Oscillatory zoned cores show a concordant age spectrum between 520 and 650 Ma, with some isolated grains with ages of 890 and 1790 Ma. Rims yield early Ordovician ages as well as younger ages of 350 and 400 Ma. Although some of these analyses are highly discordant due to the small size of the crystals, these data loosely constrain migmatite development to the Early Carboniferous.

WSB. Four samples from the WSB (fig. 3) were analyzed by the U-Pb zircon LAM-ICP-MS (two samples) and by SHRIMP (two samples). Three of the samples, CM-112 (9°32′34″S, 76°38′34″W), CM-116U (9°47′07″S, 76°4′19″W), and CM-133 (9°49′16″S, 76°34′17″W) are muscovite-albite-quartz schists. The other sample, CM-158 (9°51′22″S, 76°24′26″W) is a meta-arenite, with porphyroclasts of K-feldspar, muscovite and biotite, and a foliation defined by small white micas.

Zircons from the four samples are mainly prismatic, with some abrasion on the rim tips, probably due to sedimentary transport. CL imaging on some of the samples show predominantly oscillatory zoned zircons with lesser homogenous and sector zoned ones. U/Th ratios of most of these zircons

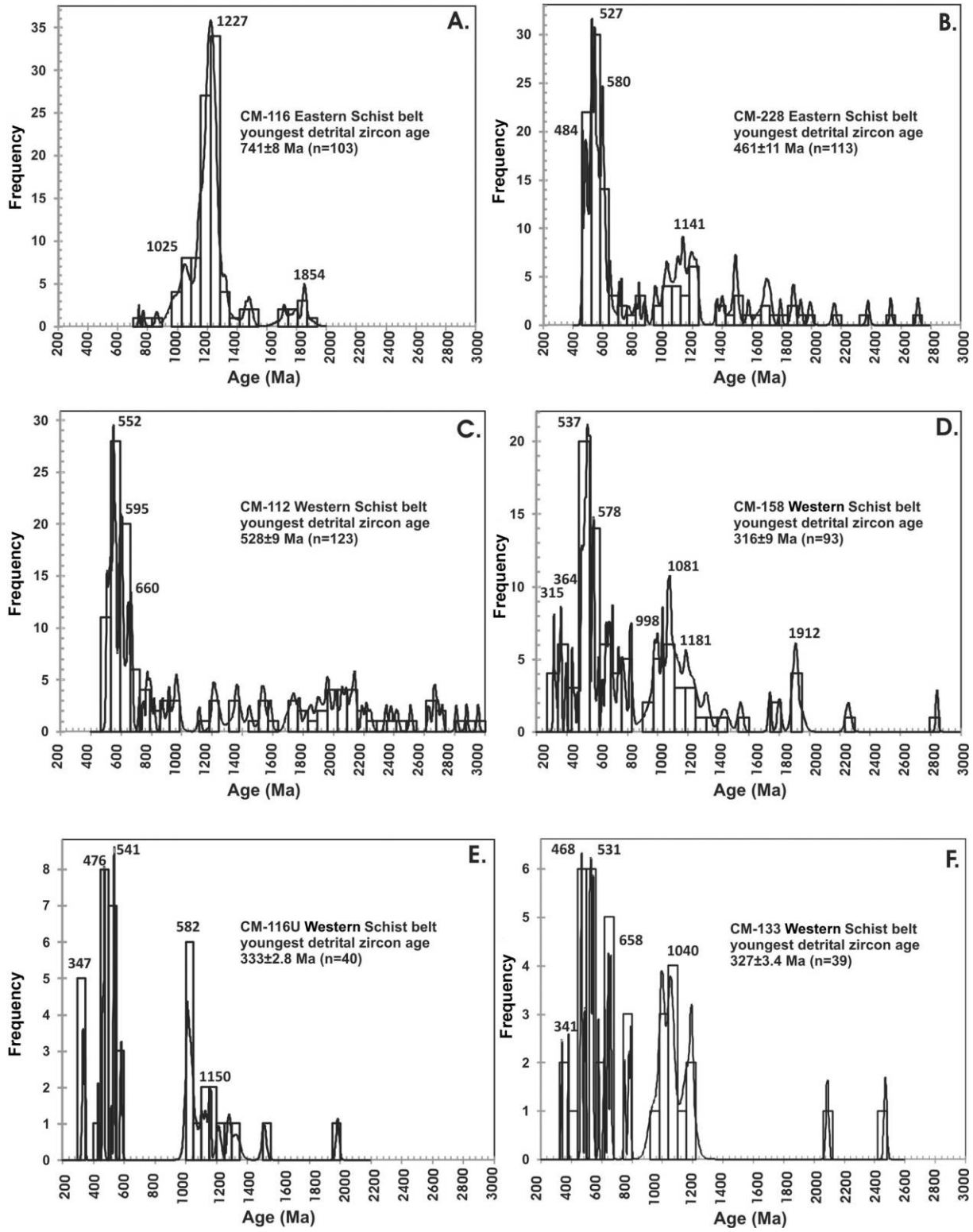

Figure 5. U-Pb detrital zircon histograms from metasedimentary rocks of the eastern and western schist belts. *A*, CM-116; *B*, CM-228; *C*, CM-112; *D*, CM-158; *E*, CM-116U; *F*, CM-133.

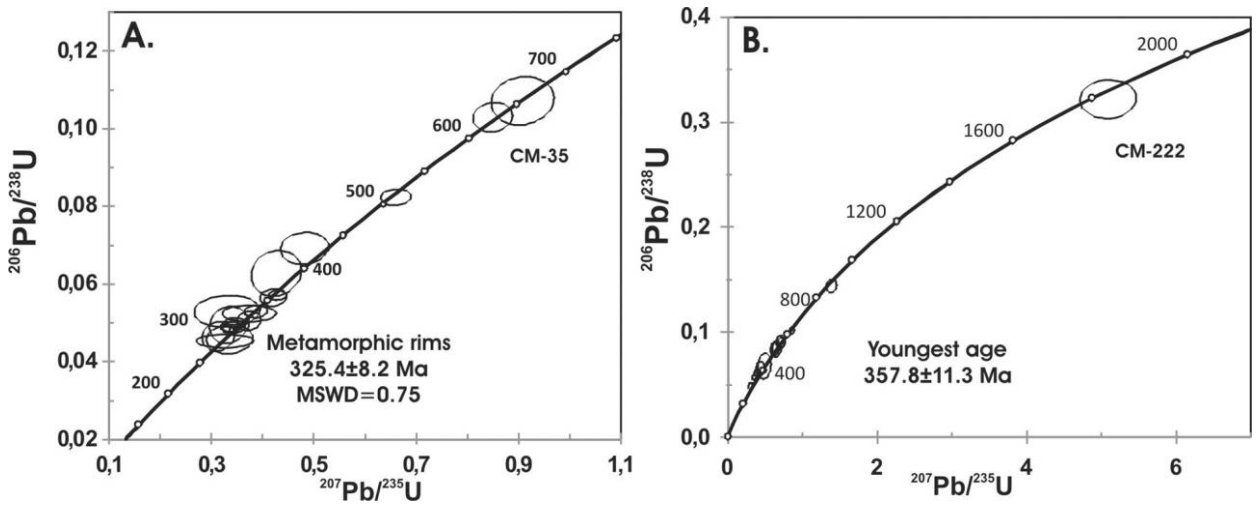

Figure 6. U-Pb concordia diagrams from migmatite samples CM-35 (*A*) and CM-222 (*B*).

are <12 suggesting a typical magmatic origin (Vabra et al. 1999; Rubatto et al. 2002).

LAM-ICP-MS analysis of 123 zircons from sample CM-112 exhibits a quasi-continuous age spectra between 500 and 2800 Ma (fig. 5*C*). There is a prominent $^{206}Pb/^{238}U$ age population between 500 and 660 Ma ($n = 63$) and a lesser one at 1700–2400 Ma ($n = 26$). Older Archean zircons were also found, including four grains that yield a weighted mean average age of 2670 ± 61 (2σ).

Sample CM-158 ($n = 93$), dated by the same method, yields mostly concordant zircon ages (fig. 5*D*) in two continuous intervals from between 310 and 800 Ma and between 900 and 1420 Ma ($n = 85$). The youngest concordant zircon has a $^{206}Pb/^{238}U$ age of 317 ± 7 Ma. Although older zircons are apparently less concordant, they point to the presence of Paleoproterozoic and Archean material in the source region. The most abundant subpopulation ($n = 44$) yields ages between 480 and 640 Ma, whereas there is another minor population of 13 grains with ages in the 310–480 Ma range. There are also age groups of 640–800 Ma ($n = 15$) and 900–1420 Ma ($n = 22$).

Zircons from sample CM-116U were analyzed by SHRIMP, and CL images were obtained in order to select specific spots on the grains. Five of the zircons show concordant Late Paleozoic $^{206}Pb/^{238}U$ ages between 324 and 356 Ma (fig. 5*E*), whereas the other 19 define an age interval between 432 and 591 Ma, (with small peaks at 477, 539, and 582 Ma). Another group of 14 zircons yields Mesoproterozoic ages between 1000 and 1370 Ma, and the last two zircon analyses yield concordant $^{207}Pb/^{206}Pb$ ages of 1936 ± 19 and 1442 ± 14 Ma.

Sample CM-133 was also analyzed by SHRIMP. The youngest three zircons from this sample yield concordant ages, with two grains defining a mean $^{206}Pb/^{238}U$ age of 337.2 ± 2.3 Ma (2σ) and the third yielding 385 ± 4 Ma. (fig. 5*F*). The dominant population includes 22 zircons with ages in the 460–720-Ma time interval, with peaks at 468, 530, and 645 Ma. Eleven zircons yield single ages between 850 and 1300 Ma. Finally, there is a minor subpopulation that yields Paleoproterozoic ages of 2461 ± 28 and 2081 ± 22 Ma.

Nd Isotopes. Whole-rock samples for Sm-Nd isotopic analysis were selected to cover the spectrum of lithologies in the ESB and the WSB. Twelve samples from the eastern belt and six from the western belt were analyzed (table A2; fig. 3). All samples were thoroughly screened for weathered portions and veining.

In order to check for possible postdepositional alteration, $f_{Sm/Nd}$ versus ε_{Nd} was evaluated for the time of deposition of the sedimentary protolith (Bock et al. 1994; Cullers et al. 1997). Both belts yield values typical of a sedimentary trend (fig. 7, *left*), with just one of the samples (CM-83) yielding an $f_{Sm/Nd}$ of 0.19, suggesting some fractionation during metamorphism. Therefore, the results are considered to reveal significant information on the provenance of the sedimentary protoliths.

Depositional ages for the two metasedimentary belts were estimated based on the youngest detrital zircon ages, stratigraphical relationships with ov-

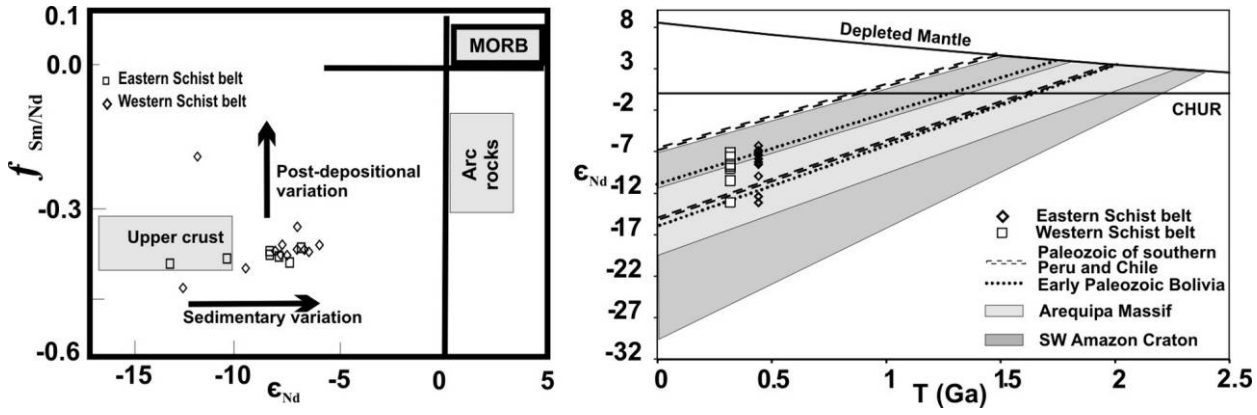

Figure 7. *Left*, $f_{Sm/Nd}$ versus ε_{Nd} diagram for evaluation of postdepositional alteration (Bock et al. 1994). *Right*, Sm-Nd envelopes from the eastern and western schist belts compared with other provinces and tectonic domains.

erlying Paleozoic sedimentary units, intrusive relationships, and constraints on the timing of metamorphism. For the ESB, the youngest detrital zircon has a $^{206}Pb/^{238}U$ age of 440 Ma, Ar-Ar muscovite metamorphic ages are ca. 420 Ma, and the oldest intrusive rock has yielded K-Ar amphibole ages of ca. 360 Ma (Cardona et al. 2007). For the WSB, the youngest detrital zircon age is ca. 320 Ma, and K-Ar muscovite ages are ca. 300 Ma (Cardona 2006). Lower Permian sediments are deposited over the western schists. Taking all this into account, 430 Ma and 310 Ma are considered to be close to the probable depositional ages of the eastern and western belts, respectively. Variations up to ±30 Ma will be practically negligible for the calculated ε_{Nd} values.

The lower- and higher-grade metasediments of the ESB schists yield negative $\varepsilon_{Nd\,(430\ Ma)}$ values between −6.3 and −12.5 (fig. 7, *right*), whereas samples from the WSB also yield similar $\varepsilon_{Nd(320\,Ma)}$ values in the −7.1 to −13.2 interval. Sm-Nd T_{DM} model ages were calculated after De Paolo et al. (1991) to account for minor Sm/Nd fractionation, and they yield values between 1.7 and 2.1 Ga for the ESB and 1.6–2.0 Ga for the WSB (fig. 4*B*).

The negative ε_{Nd} values from both metasedimentary belts suggest the presence of old, highly differentiated source areas. Moreover, the variations in T_{DM} model ages and ε_{Nd} values reflect the existence of mixed components of different age (cf. Goldstein et al. 1997; Bock et al. 2000). The great similarity of the Nd isotopic signature of the two belts together with the detrital zircon data also suggests that they shared the same sources. Values in the same range were obtained by Macfarlane (1999) and Haeberlin (2002) at close to latitude 8°S, within metamorphic rocks also ascribed to the Marañon Complex.

The Nd isotopic evolution trend of the Marañon Complex (fig. 7, *right*) overlaps with that of the southwest Amazonian Craton (Cordani et al. 2000). Sm-Nd model ages of the Marañon Complex are similar to crystallization ages of igneous rocks of the Rondonian San Ignacio and Sunsas provinces of the Amazonian Craton that were formed between 1.0 and 1.5 Ga (Tassinari et al. 2000). Such an isotopic signature is also similar to the one of the Paleozoic sequences of the Bolivian and Chilean Andes (fig. 7, *right*), which yield Sm-Nd T_{DM} model ages of 1.6–2.2 Ga and ε_{Nd} values between −6 and −11 (Lucassen et al. 2000; Egenhoff and Lucassen 2003).

Grenvillian-age basement from the coastal Arequipa massif in southern Peru presents slightly older T_{DM} values, between 1.9 and 2.3 Ga (Loewy et al. 2004), whereas the basement inliers of the northern Colombian Andes yield consistent Sm-Nd model ages of 1.6–1.9 Ga (Cordani et al. 2005).

Tectonostratigraphic Constraints. The geochronology results reported above provide a new tectonostratigraphic framework for the Marañon Complex at 10°S (fig. 8). U-Pb zircon dating implies a ~613-Ma magmatic event within Grenvillian-type basement. This basement was affected by an amphibolite-facies metamorphic episode at 484 ± 12 Ma, as indicated by the crystallization of overgrowths of metamorphic zircon, and was intruded by granitoids at 468 ± 2 Ma. Subsequently two volcano-sedimentary basins were laid down. The first was metamorphosed in the Middle Paleozoic, and

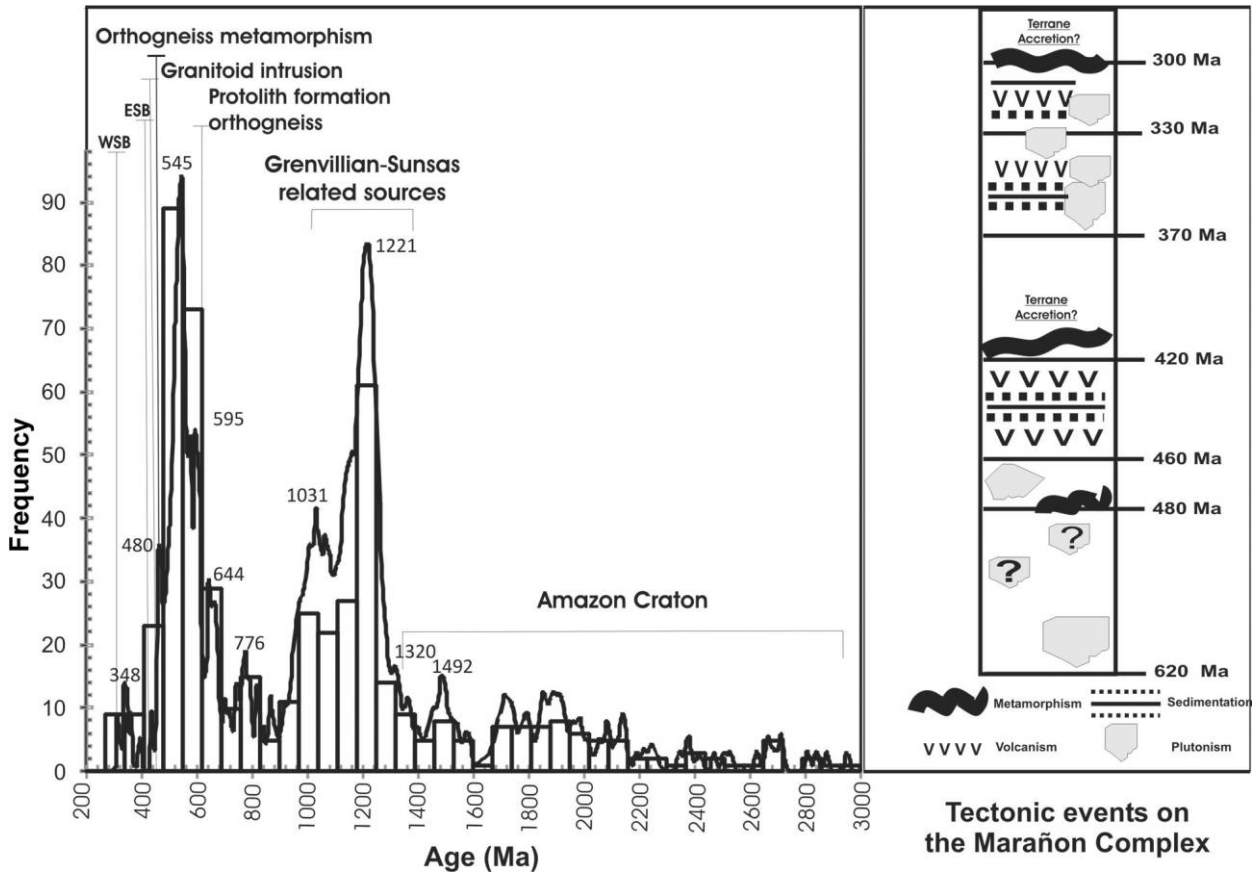

Figure 8. Schematic tectonic evolution of the Marañon Complex. *ESB* = Eastern Schist Belt, *WSB* = Western Schist Belt.

the second one was in the Late Paleozoic. Their depositional history is constrained by their youngest detrital zircons, the timing of metamorphism in both units, and their stratigraphic relationships with the overlying strata. Sedimentation is constrained to 450–420 and 318–300 Ma for the ESB and WSB, respectively.

We attribute the greenschist-facies mylonitic event affecting the Ordovician granitoid and orthogneiss to the early Paleozoic deformational event of the ESB. A younger (Late Carboniferous to Early Permian) deformational event is also recorded in the ESB. It is related to the formation of a crenulation cleavage and partial resetting of the isotopic systems (Cardona et al. 2007) as well as the generation of migmatites spatially related to granitoid intrusions.

U-Pb detrital zircon results provide additional tectonostratigraphic constraints: (1) both eastern and western belts contain zircon grains that can be temporally related to the immediately preceding geological events; (2) the youngest detrital zircon age is marginally older than the inferred depositional age; (3) a subpopulation of the zircon age spectra correlates with the crystallization ages of the orthogneisses and mylonitised plutonic rocks; (4) zircons are of predominantly magmatic character as evidenced by the U/Th ratios and the predominance of oscillatory zoning in CL images; and (5) there is a gap in the Paleozoic detrital record between 440 and 390 Ma. Such data suggest that some of these tectonomagmatic events are regionally widespread and that the growth of both younger basins was contemporaneous with magmatic activity. The continuous cannibalism within this orogenic belt, together with the presence of Mesoproterozoic and older detrital zircon ages within the schists, and inherited zircon ages within plutons, as well as the similar Nd isotopic signatures (negative ε_{Nd} and Paleoproterozoic Sm-Nd T_{DM} model ages) of the two schist belts, indicate that they formed on an active continental margin deposited over old continental crust.

When the U-Pb detrital zircon data are compared

with the Sm-Nd whole-rock results, only 16% of the analyzed zircons yield crystallization ages older than the Proterozoic whole-rock Sm-Nd model ages. This trend may reflect a detrital contribution of siliciclastic particles other than zircon, possibly including rare earth element–rich phases such as epidote or monazite (Goldstein et al. 1997; Dickin 2000). However, we consider that it is more feasible that the younger Paleozoic and Neoproterozoic magmatic sources formed in a magmatic arc setting characterized by substantial contamination by older crust during its formation, as has been shown to be a common feature within the central Andes (Lucassen et al. 2004).

In the case of the Neoproterozoic to Ordovician geological record, the existence of well-defined phases of magmatic activity, together with continuous zircon detrital input between 660 and 450 Ma, is compatible with an active margin setting (figs. 8, 9*A*). The 480-Ma zircon overgrowths in the orthogneiss are probably also linked to phases of magmatism in such a continental arc environment (fig. 9*B*). This tectonomagmatic event has been recorded along most of the eastern Peruvian Andes, including the northern and southern segments of the Marañon Complex (Chew et al. 2007*b*) and the Arequipa massif in southern Peru, where syn- and post-tectonic granitoids were emplaced between 472 and 460 Ma (Loewy et al. 2004). Additionally, in the southern segment of the Eastern Cordillera of Peru, close to the city of Cuzco, Bahlburg et al. (2006) have demonstrated the existence of an Ordovician back-arc setting. A similar Paleozoic tectonic configuration apparently exists along much of the proto-Andean margin, as seen by the presence of the Puna and Famatinian magmatic arcs in the Chilean and Argentinean Andes (Bahlburg and Hervé 1997; Pankhurst and Rapela 1998; Ramos 2000), and by the presence of Ordovician-Silurian magmatic and deformational events in the northern Andes (Burkley 1976; Restrepo-Pace 1995; Ramos and Aleman 2000).

The next major tectonomagmatic activity corresponds to the Silurian regional metamorphic

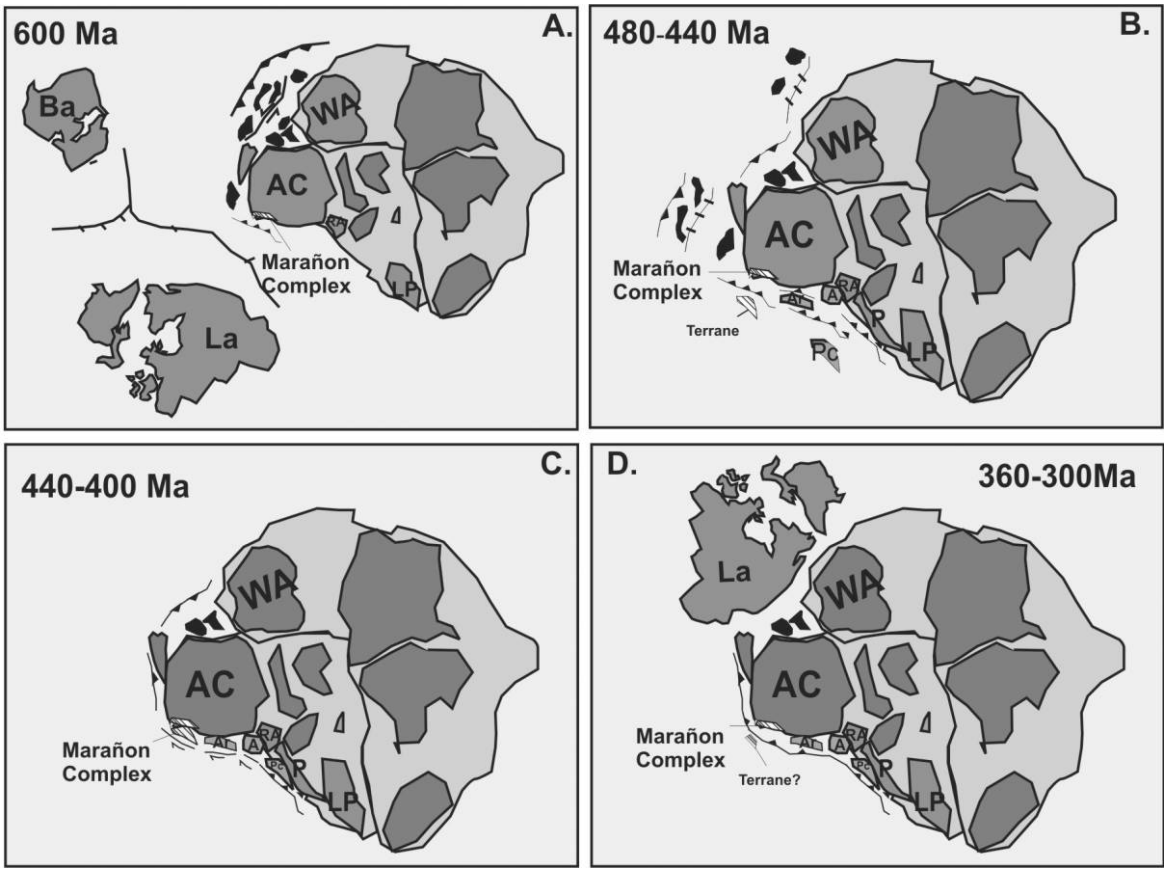

Figure 9. Paleogeography of the western margin of the Amazonian Craton (including the Marañon Complex) between 600 and 300 Ma (modified from Cawood et al. 2001; Murphy et al. 2004*a*; Cordani et al. 2005.)

event recorded by the ESB and by the reworked Ordovician magmatic basement. It also coincides with a major gap in the magmatic record between 440 and 390 Ma, a feature that has been documented in other segments of the Eastern Cordillera of Peru (Chew et al. 2007*b*) as well as in northern Chile (Bahlburg and Hervé 1997; Bahlburg and Vervoort 2007). Recently Ramos (2008*a*) reviewed the available evidence for possible terrane accretion along the Peruvian margin. He considered that the Paracas terrane was accreted to the Peruvian margin during the Ordovician. Alternatively, we suggest that this event may be slightly younger and may be represented by the Silurian medium-pressure, Barrovian-type regional metamorphism within the ESB (fig. 9*C*).

The restricted Silurian and the Devonian magmatic activity that followed the mentioned accretionary event may be related to a change in plate vectors, or to an oblique convergent margin with restricted magmatic activity (fig. 9*C*). In contrast, several terrane-related accretionary events have been documented in other segments of the Andean belt in Argentina, Chile, and Colombia in Silurian and Devonian time (Thomas and Astini 1996; Ramos 2000, 2004; Ordóñez-Carmona et al. 2006). Moreover, in the Chilean Andes there is evidence of a passive margin environment during this time interval (Bahlburg and Hervé 1997; Bahlburg and Vervoort 2007).

Magmatic arc activity was reestablished in the Carboniferous, as evidenced by the U-Pb detrital record, the volcanic protoliths of the western schists, andesite flows associated with the Mississipian Ambo Group (Dalmayrac et al. 1988), the U-Pb migmatite ages reported in this study, and K-Ar amphibole and biotite ages of between 356 and 291 Ma (Cardona 2006). This activity is widespread along the central and northern segments of the Eastern Cordillera of Peru (Chew et al. 2007*b*; Miskovic et al. 2005, Miskovic and Schaltegger 2008).

The end of the Late Paleozoic tectonic cycle is marked by a major regional metamorphic event of Late Carboniferous–Early Permian age that affects the western belt and produces the development of a crenulation cleavage within the eastern belt (Cardona et al. 2007). This metamorphic episode may be connected with an apparent shutoff in magmatic activity (fig. 9*D*). It is also expressed farther south in central Peru by the development of syntectonic migmatites at ca. 310 Ma (Chew et al. 2007*b*) and in northern Peru by deformation of Carboniferous granitoids along major shear zones (Haeberlin 2002). Terrane accretion, or changes in the subduction configuration may have caused the inversion of the arc-related basins (Hervé et al. 1995; Collins 2002; Stern 2002; Cawood and Buchan 2007). The actual position of the Carboniferous continental magmatic arc more than 350 km from the paleotrench (V. A. Ramos, pers. comm., 2007) can be explained with the accretion of a terrane that causes the widening of the continental margin. The late Paleozoic "Gondwanide" orogeny has been also documented in the Chilean Andes, where Late Carboniferous turbiditic sequences are deformed and are associated with the evolution of a subduction complex (Bahlburg and Hervé 1997; Willner et al. 2005). In the Eastern Cordillera of the Bolivian Andes, a major deformational event between 290 and 320 Ma has been recognized (Jacobshagen et al. 2002), while in the Argentinean Andes, a similar deformational event has been envisaged for the Early Permian, as a consequence of a flat-slab subduction process (Ramos 2008*b*). Within the northern Andes (Ecuador, Colombia, Venezuela) a few suites of syntectonic granitoids and some metamorphic belts have been linked to the accretion of continental terranes associated with the formation of Pangaea and with the evolution of subduction of the proto-Pacific lithosphere (Ramos and Aleman 2000; Vinasco et al. 2006; Cardona et al. 2008).

Following the orogenic phases, a period of major extension with basin formation and bimodal magmatism was installed along most of the Andes (Kontak et al. 1985, 1990; Ramos 2000; Franzese and Spalletti 2001; Sempere et al. 2002; Miskovic et al. 2005). This latter extensional process has been related to a change in the convergence velocity between the Pacific and South American plates during the final assembly of Pangea, with the consequent orogenic collapse of the Late Paleozoic orogen (Gurnis 1988; Ramos and Aleman 2000).

Provenance of the Marañon Complex. The U-Pb detrital zircon ages of the metamorphic rocks of the Marañon Complex indicate contributions from at least four main sources: Carboniferous-Ordovician (n = 48 U-Pb detrital zircon analyses), Cambrian–Middle Neoproterozoic (n = 207), Late Neoproterozoic–Mesoproterozoic (n = 190), and an older discontinuous record that extends until 2.95 Ga (n = 66). As discussed above, the Neoproterozoic and Paleozoic sources must be related to the continuous reworking of the continental margin, while contemporaneous arc magmatism was in action. Taking into account the great similarities in detrital zircon populations observed in the different units of the Marañon Complex, we used the entire detrital record of the Marañon Complex to constrain further the provenance regions of the Cambrian to Proterozoic detritus (fig. 8).

Zircons older than Mesoproterozoic (including some Archean) can be attributed to several geological provinces in the Amazonian Craton (Tassinari et al. 2000). Moreover, the Sm-Nd T_{DM} model ages between 1.6 and 2.1 Ga are also comparable with those of the granitoids of the Rondonian San Ignacio and Rio Negro–Juruena belts of the Amazonian Craton and those of the Proterozoic inliers in the northern Andes (Cordani et al. 2000, 2005; Loewy et al. 2004; Cordani and Teixeira 2007).

A significant zircon population is encountered between 1.3 and 0.90 Ga ($n = 156$) with major peaks at 1030, 1230, and 1320 Ma. These ages reflect tectonomagmatic episodes related to Grenvillian-type orogens that culminated with the juxtaposition of Laurentia and Baltica with the Amazon Craton, in the process of agglutination of Rodinia (Hoffman 1991). Proximal sources for these might be the Rondonian San Ignacio and Sunsas provinces of the Amazonian Craton (Litherland et al. 1989; Tassinari et al. 2000; Cordani and Teixeira 2007). Alternative sources are a few Proterozoic basement inliers found along the northern Andean belt, in Colombia and Venezuela (Cordani et al. 2005). In Peru, two Grenvillian domains have been recognized. First, the Arequipa Massif, characterized as major terrane including magmatic and high-grade metamorphic rocks with 0.97–1.2 Ga (Wasteneys et al. 1995; Loewy et al. 2004; Chew et al. 2007*a*). Second, in the southeastern part of the Peruvian Amazon basin, there is an isolated massif of granulite that has yielded a U-Pb age of 1140 ± 23 Ma (Dalmayrac et al. 1988).

The above evidence seems to imply that a major Grenvillian-related domain extends along this segment of the western margin of Gondwana, including the central Peruvian and Colombian Andes. Moreover, if we consider the position of the Rondonian San Ignacio orogenic belts at the southwestern edge of the Amazonian Craton, we envisage that this Grenvillian domain may continue also under the Acre and Solimões sedimentary basins.

The Neoproterozoic crystallization age of the CM-80 orthogneiss protolith falls within the age interval of the Cambrian to Neoproterozoic detrital zircon ages ($n = 207$) whose major peaks are at 545, 595, and 645 Ma. This population is the most abundant in the detrital record in other segments of the eastern Peruvian Andes, south of Lima (Chew et al. 2007*a*, 2008). It is of special interest, as the role of the proto-Andean margin in relation with the processes of Rodinian fragmentation and subsequent Gondwana assembly is poorly understood (Pankhurst and Rapela 1998; Chew et al. 2008). Critical issues that must be considered in order to constrain the source of this detrital population include the following: (1) the age-equivalent Brasiliano orogens at the eastern margin of Amazonia are far removed from the proto-Andean margin; (2) within the western Amazon Craton, tectonomagmatic events within this time period have not been found (Tassinari et al. 2000); (3) although Neoproterozoic rift-related magmatism is relatively common on the Laurentia and Baltica margins during Rodinia breakup (e.g., Tollo et al. 2004), it is predominantly mafic in character, and hence, its involvement as a major detrital zircon source to proto-Andean sedimentary sequences is likely to be limited (Cawood et al. 2001; Bream et al. 2004; Thomas et al. 2004; Carter et al. 2006).

It is commonly assumed that separation between Laurentia and Amazonia took place at about 570 Ma, whereas between Laurentia and Baltica it was around 600 Ma (Bingen et al. 1998; Cawood et al. 2001; Kinny et al. 2003). We consider that the extensive Neoproterozoic detrital record at the western margin of Gondwana must be related to a major felsic-intermediate magmatic source that is more likely to have an arc affinity, and therefore, an alternative tectonic scenario could be an earlier separation between Amazonia and Baltica-Laurentia followed by the installation of an active margin operated by subduction since at least 640 Ma. This continental arc is considered to be the major feeder of the extensive Neoproterozoic to Cambrian zircon found in the Marañon schist belts. This inferred Neoproterozoic subduction phase started earlier than those already envisaged for Laurentia, Baltica, and other segments of the proto-Andean margin, considered respectively at 500, 550–560, and 600 Ma (Rapela et al. 1998; Van Staal et al. 1998; Cocks and Torsvik 2005; Escayola et al. 2007). However, the 640 Ma subduction process would be contemporaneous with the initiation of subduction-related magmatism on several peri-Gondwana terranes, including the southernmost Pampean terrane of the proto-Andean margin (Murphy et al. 2004; Escayola et al. 2007)

Another consequence of this tectonic configuration is the potential connection with several peri-Gondwanan terranes such as Avalonia, Ganderia, Carolinia, and Iberia. These terranes formed as intraoceanic and continental arcs and yield U-Pb and Sm-Nd isotopic signatures that might place them in the vicinity of the Amazonian Craton at the northwest margin of Gondwana from 650 Ma until the Cambro-Ordovician when they departed (Keppie et al. 1998; Murphy et al. 2000, 2004*a*; Gutierrez-Alonso et al. 2003; Ingle et al. 2003; Collins and Buchan 2004; Carter et al. 2006; Reusch et al. 2006;

Rogers et al. 2006). Concrete evidence of the accretion of these terranes to the continental margin is still scarce. However, examples may be found in the Venezuelan Andes, where syntectonic Neoproterozoic granitoids associated with a low- to medium-grade metamorphic event are reported from the Bella Vista Group (Burkley 1976; Ramos and Aleman 2000). If these terranes were accreted during the Neoproterozoic, they might provide a mechanism for the structural inversion of the passive margin of the Amazonian Craton that must have formed after the Rodinia breakup. The detrital zircon populations of the Peruvian segment of the proto-Andean margin are also comparable with the detrital zircon record of these peri-Gondwanan terranes (Keppie et al. 1998; Murphy et al. 2000, 2004*b*; Gutierrez-Alonso et al. 2003; Ingle et al. 2003; Collins and Buchan 2004; Carter et al. 2006; Reusch et al. 2006; Rogers et al. 2006), which also indicates a possible connection.

Paleogeographic studies from central Peru have suggested that a terrane with continental basement was located against the western margin of the Eastern Cordillera, bounded to the east by the Marañon Complex (see reviews by Ramos and Aleman 2000; Ramos 2008*a*). This inferred terrane, termed "Paracas," has been considered a conjugate margin to the Oaxaquia terrane (Ramos and Aleman 2000; Ramos 2008*a*), a major Gondwanan Mesoproterozoic domain with an Ordovician sedimentary cover that forms the southern portion of Mexico (Ortega-Gutierrez et al. 1995; Keppie and Ortega-Gutiérrez 1999). However, the Nd isotope record from Oaxaquia and the U-Pb detrital record from its younger Paleozoic cover sequences (Weber and Köhler 1999; Gillis et al. 2005) do not exhibit the strong Neoproterozoic to Cambrian signature found within the Marañon segment of the Proto-Andean margin. Recent reviews of Rodinian paleogeography have questioned the Peruvian connection with the Oaxaquia microcontinent (Keppie and Dostal 2007). Although the position of the conjugate terrane remains uncertain, we think that a major terrane dispersion event took place during the Neoproterozoic, either associated with Rodinia breakup or with the departure of Avalonia-Cadomia-type terranes. Young south to north Meosozic dispersion events are also possible, as suggested by recent paleomagnetic data from the Colombian Andes (Bayona et al. 2006).

Conclusions

1. Lithostratigraphic evidence, U-Pb zircon geochronology and Nd isotopic data from the Marañon Complex at 10°S in the Eastern Cordillera of the Peruvian Andes provide a tectonostratigraphic framework for the proto-Andean margin from the Neoproterozoic until the Late Carboniferous. These include development of an arc since 620 Ma or earlier that lasted until the Silurian, while a major metamorphic event occurred at about 480 Ma.

2. Two separate volcano-sedimentary basins formed within an arc-related setting. The older basin was deformed and metamorphosed during the Middle Silurian under regional (Barrovian) metamorphic conditions that may have been related to ocean closure and a terrane accretionary event. The younger basin was formed during the Carboniferous, and its inversion at around 300–310 Ma may be related to either a terrane accretionary event or to a change in subduction dynamics. In between the deposition of these two basins there is a Silurian to Devonian gap in the magmatic record. This tectonic evolution is part of the long-lived peri-Gondwanan Terra Australis orogen that commenced after the separation between Laurentia and Godwana. It evolved by subduction of the proto-Pacific ocean and lasted until the Gondwanide-Alleghenian orogenic events that culminated in the assembly of Pangaea (Cawood 2005).

3. Provenance constraints based on U-Pb detrital zircon data have shown that this margin grew on the edge of the Amazonian Craton, and was proximal to major orogenic belts of Grenvillian and Brasiliano age. The presence of a Neoproterozoic orogenic belt at the proto-Andean margin suggests an earlier fragmentation of the margins of Gondwana with Baltica and Laurentia (Chew et al. 2008) and a possible connection with several Peri-Gondwanan arc-related terranes.

4. The Paleoproterozoic Sm-Nd T_{DM} model ages contrast with the younger U-Pb zircon detrital ages and indicate that recycling of older crust was an important element in the Mesoproterozoic, Neoproterozoic, and Early Paleozoic evolution of the Peruvian segment of the proto-Andean margin.

5. The growth of this active convergent margin results from several stages of subduction as well as terrane accretion and dispersion. Whereas some events may be of local character, the synchronicity with similar events along the Andean chain may reflect a more regional-scale plate tectonic control (Cawood and Buchan 2007; Ramos 2008*a*).

ACKNOWLEDGMENTS

We wish to acknowledge the support received from the São Paulo State Research Agency (FAPESP), grant 02/072488-3. We thank the colleagues and the

staff of the Geochronological Research Center of the University of São Paulo for technical help and fruitful discussions. J. Macharé and O. Palacios of the Peruvian Geological Survey (INGEMMET) are acknowledged for their logistical support and help provided during several stages of this research. A. Zapata and J. Galdos of INGEMMET are acknowledged for discussions and help during field work. Thorough and clear reviews and suggestions by V. A. Ramos, J. Aleinikoff, and A. Anderson are acknowledged. The assistance of M. Marulanda during field work and other stages of this research is deeply appreciated. These results are part of A. Cardona's PhD thesis at the University of São Paulo.

REFERENCES CITED

Bahlburg, H. 1993. Hypothetical southeast Pacific continent revisited: new evidence from the middle Paleozoic basins of northern Chile. Geology 21:909–912.

Bahlburg, H.; Carlotto, V.; and Cárdena, J. 2006. Evidence of Early to Middle Ordovician arc volcanism in the Cordillera Oriental and Altiplano of southern Peru, Ollantaytambo Formation and Umachiri beds. J. S. Am. Earth Sci. 22:52–65.

Bahlburg, H., and Hervé, F. 1997. Geodynamic evolution and tectonostratigraphic terranes of northwestern Argentina and northern Chile. Geol. Soc. Am. Bull. 109: 869–884.

Bahlburg, H., and Vervoort, J. D. 2007. LA-ICP-MS geochronology of detrital zircons in Late Paleozoic turbidite units of northern Chile: implications for terrane processes. Goldschmidt Conf. Abstr. 71 15S:A51.

Basei, M. A. S.; Siga, O., Jr.; Sato, K.; and Sproeser, W. M. 1995. A instalação da metodologia U-Pb na universidade de São Paulo. An. Acad. Bras. Cienc. 67:221–237.

Bayona, G.; Rapalini, V.; and Costanzo-Alvarez, V. 2006. Paleomagnetism in Mesozoic rocks of the northern Andes and its implications in Mesozoic tectonics of northwestern South America. Earth Planets Space 58: 1–18.

Benavides-Cáceres, V. 1999. Orogenic evolution of the Peruvian Andes: the Andean cycle. In Skinner, J., ed. Geology and ore deposits of the central Andes. Soc. Econ. Geol. Spec. Publ. Ser. 7, p. 61–107.

Bingen, B.; Demaiffe, D.; and van Breemen, O. 1998. The 616 Ma old Egersund basaltic dyke swarm, SW Norway, and Late Neoproterozoic opening of the Iapetus Ocean. J. Geol. 106:565–574.

Bock, B.; Bahlburg, H.; Wörner, G.; and Zimmermann, U. 2000. Tracing crustal evolution in the southern central Andes from Late Precambrian to Permian with geochemical and Nd and Pb isotope data. J. Geol. 108: 515–535.

Bock, B.; McLennan, S. M.; and Hanson, G. N. 1994. Rare element redistribution and its effects on the neodymium isotope system in the Austin Glen Member of the Normanskill Formation, New York, USA. Geochim. Cosmochem. Acta 58:5245–5253.

Bream, B. R.; Hartcher, R. D.; Miller, C. F.; and Fullagar, P. D. 2004. Detrital zircon ages and Nd isotopic data form the southern Appalachian crystalline core, Georgia, South Carolina, North Carolina and Tennessee: new provenance constraints for part of the Laurentian Margin. Geol. Soc. Am. Mem. 197:459–474.

Burkley, L. A. 1976. Geochronology of the central Venezuelan Andes. PhD dissertation, Case Western Reserve University, Cleveland, 150 p.

Cardona, A. 2006. Reconhecimento da evolução tectônica da proto-margem Andina do centro-norte Peruano, baseada em dados geoquímicos e isotópicos do embasamento da Cordilheira Oriental na região de Huánuco-La Unión. PhD thesis, Universidade de São Paulo. 247 p.

Cardona, A.; Cordani, U.; and Nutman, A. 2008. U-Pb SHRIMP zircon, $^{40}Ar/^{39}Ar$ geochronology and Nd isotopes from gneissic and granitoid rocks of the Illescas massif, Perú: a southern extension of a fragmented Late Paleozoic orogen? *In* VI South American Symposium on Isotope Geology, San Carlos de Bariloche, Argentina. Extended abstracts.

Cardona, A.; Cordani, U.; Ruiz, J.; Valencia, V.; Nutman, A.; and Sanchez, A. 2006. U-Pb detrital zircon geochronology and Nd isotopes from Paleozoic meta-sedimentary rocks of the Marañon Complex: insights on the proto-Andean tectonic evolution of the eastern Peruvian Andes. *In* Proceedings, V South American Symposium on Isotope Geology, Punta del Este, Uruguay, p. 208–211.

Cardona, A.; Cordani, U.; and Sanchez, A. 2007. Metamorphic, geochronological and geochemical constraints from the pre-Permian basement of the eastern Peruvian Andes (10°S): a Paleozoic extensional-accretionary orogen? 20th Colloquium on Latin American Earth Sciences, April 11–13, Kiel, Germany. Abstracts, p. 29–30.

Carter, B. T.; Hibbard, J. P.; Tubrett, M.; and Sylvester, P. 2006. Detrital zircon geochronology of the Smith River Allochthon and Lynchburg Group, southern Appalachians: implications for Neoproterozoic-Early Cambrian paleogeography. Precambrian Res. 147:279–304.

Cawood, P. A. 2005. Terra Australis Orogen: Rodinia breakup and development of the Pacific and Iapetus margins of Gondwana during the Neoproterozoic and Paleozoic. Earth Sci. Rev. 69:249–279.

Cawood, P. A., and Buchan, C. 2007. Linking accretionary orogenesis with supercontinent assembly. Earth Sci. Rev. 82:217–256.

Cawood, P. A.; McCausland, P. J. A.; and Dunning, G. R. 2001. Opening Iapetus: constraints from the Lauren-

tian Margin in Newfoundland. Geol. Soc. Am. Bull. 113:443–453.

Chew, D. M.; Kirkland, C. L.; Schaltegger, U.; and Goodhue, R. 2007*a*. Neoproterozoic glaciation in the Proto-Andes: tectonic implications and global correlation. Geology 35:1095–1099.

Chew, D. M.; Magna, T.; Kirkland, C. L.; Miskovic, A.; Cardona, A.; Spikings, A.; and Schaltegger, U. 2008. Detrital zircon fingerprint of the Proto-Andes: evidence for a Neoproterozoic active margin? Precambrian Res. 167:186–200.

Chew, D. M.; Schaltegger, U.; Kosler, J.; Whitehouse, M. J.; Gutjahr, M.; Spikings, R. A.; and Miskovic, A. 2007*b*. U-Pb geochronologic evidence for the evolution of the Gondwanan margin of the north-central Andes. Geol. Soc. Am. Bull. 119:697–711.

Cobbing, E. J., and Sanchez, A. W. 1996*a*. Mapa geológico del cuadrángulo de La Unión, 20J. Lima, Peru, Instituto Geológico Minero y Metalúrgico.

———. 1996*b*. Mapa geológico del cuadrángulo de Yanahuanca, 21J. Lima, Peru, Instituto Geológico Minero y Metalúrgico.

Cocks, R. L., and Torsvik, T. H. 2005. Baltica from the late Precambrian to mid-Palaeozoic times: the gain and loss of a terrane's identity. Earth Sci. Rev. 72:39–66.

Collins, A., and Buchan, C. 2004. Provenance and age constraint of the South Stack Group, Anglesey, UK: U-Pb SIMS detrital zircon data. J. Geol. Soc. Lond. 161: 743–746.

Collins, W. J. 2002. Hot orogens, tectonic switching, and creation of continental crust. Geology 30:535–538.

Cordani, U. G.; Cardona, A.; Jimenez, D.; Liu, D.; and Nutman, A. P. 2005. Geochronology of Proterozoic basement inliers from the Colombian Andes: tectonic history of remmants from a fragmented Grenville belt. *In* Vaughan, A. P. M.; Leat P. T.; Pankhurst, R. J., eds. Terrane processes at the margins of Gondwana. Geol. Soc. Lond. Spec. Publ. 246:329–346.

Cordani, U. G.; Sato, K.; Teixeira, W.; Tassinari, C. C. G.; and Basei, M. A. S. 2000. Crustal evolution of the South American Platform. *In* Cordani, U. G.; Milani, E. J.; Thomaz, A., and Campos, D. A., eds. Tectonic evolution of South America. 31st International Geological Congress, Rio de Janeiro, p. 19–40.

Cordani, U. G., and Teixeira, W. 2007. Proterozoic accretionary belts in the Amazonian Craton. *In* Hatcher, R. D., Jr.; Carlson, M. P.; McBride, J. H.; and Martínez-Catalán, J. R., eds. 4-D framework of continental crust. Geol. Soc. Am. Mem. 200:297–320.

Cullers, R. L.; Bock, B.; and Guidotti, C. 1997. Elemental distributions and neodymium isotopic compositions of Silurian metasediments, western Maine, USA: redistribution of the rare earth elements. Geochim. Cosmochim. Acta 61:1847–1861.

Dalmayrac, B.; Laubacher, B.; and Marocco, R. 1988. Caracteres generales de la evolución geológica de los Andes Peruanos. Instituto Geológico Minero y Metalúrgico, Bol. 12, 313 p.

De la Cruz, J., and Valencia, M. 1996. Mapa geológico del cuadrángulo de Panao, 20L. Lima, Peru, Instituto Geológico Minero y Metalúrgico.

De Paolo, D. J.; A. M. Linn; and Schubert, G. 1991. The continental crustal age distribution: methods of determining mantle separation ages from Sm-Nd isotopic data and application to the southwestern U.S. J. Geophys. Res. 96:2071–2088.

Dickin, A. P. 2000. Crustal formation in the Grenville Province: Nd isotope evidence. Can. J. Earth Sci. 37: 165–181.

Dickinson, W. R., and Gehrels, G. E. 2003. U-Pb ages of detrital zircons from Permian and Jurassic eolianite sandstones of the Colorado Plateau, USA: paleogeographic implications. Sediment. Geol. 163:29–66.

Egenhoff, S. O., and Lucassen, F. 2003. Chemical and isotopical composition of Lower to Upper Ordovician sedimentary rocks (central Andes/South Bolivia): implications for their source. J. Geol. 111:487–497.

Escayola, M. P.; Pimental, M.; and Armstrong, R. 2007. Neoproterozoic backarc basin: sensitive high-resolution ion microprobe U-Pb and Sm-Nd isotopic evidence from the eastern Pampean ranges, Argentina. Geology 35:495–498.

Fedo, C. M.; Sircombe, K. N.; and Rainbird, R. H. 2003. Detrital zircon analysis of the sedimentary record. *In* Hanchar, J. M., and Hoskin, P. W. O., eds. Zircon: reviews in mineralogy and geochemistry. 53:277–303.

Franzese, J. R., and Spalletti, L. A. 2001. Late Triassic–early Jurassic continental extension in southwestern Gondwana: tectonic segmentation and pre-break-up rifting. J. S. Am. Earth Sci. 14:257–270.

Gehrels, G. E.; Valencia, V.; and Pullen, A. 2006. Detrital zircon geochronology by laser-ablation multicollector ICPMS at the Arizona LaserChron Center. *In* Olszewski, T.D., ed. Geochronology: emerging opportunities. Paleontol. Soc. Pap. 12:67–76.

Gehrels, G. E.; Valencia, V.; and Ruiz, J. 2008. Enhanced precision, accuracy, efficiency, and spatial resolution of U-Pb ages by laser ablation–multicollector–inductively coupled plasma–mass spectrometry. Geochem. Geophys. Geosyst., doi: 10.1029/2007GC001805.

Gillis, R. J.; Gehrels, G. E.; Ruiz, J.; and Flores de Dios, L. 2005. Detrital zircon provenance of Cambrian-Ordovician and Carboniferous strata of the Oaxaca terrane, southern Mexico. Sediment. Geol. 182:87–100.

Goldstein, S. L.; Arndt, N. T.; and Stallard, R. F. 1997. The history of a continent from U-Pb ages of zircons from Orinoco River sand and Sm-Nd isotopes in Orinoco basin river sediments. Chem. Geol. 139:269–284.

Grandin, G., and Navarro, J. 1979. Las rocas ultrabasicas en el Peru, las intrusiones lenticulares y los sills de la región de Huanuco-Monzon. Bol. Soc. Geol. Peru 63:99–115.

Gurnis, M. 1988. Large-scale mantle convection and the aggregation and dispersal of supercontinents. Nature 332:695–699.

Gutierrez-Alonso, G.; Fernández-Suárez, J.; Jeffries, T. E.; Jenner, G. A.; Tubrett, M. N.; Cox, R.; and Jackson, S. E. 2003. Terrane accretion and dispersal in the

northern Gondwana margin: an Early Paleozoic analogue of a long-lived active margin. Tectonophysics 365:221–232.

Haeberlin, Y. 2002. Geological and structural setting, age, and geochemistry of the orogenic gold deposits at the Pataz Province, Eastern Andean Cordillera, Peru. PhD thesis, University of Geneva.

Hervé, F.; Pankhurst, R. J.; Drake, R.; and Beck, M. E. 1995. Pillow metabasalts in a mid-Tertiary extensional basin adjacent to the Liquiñe-Ofqui fault zone: the Isla Magdalena area, Aysén, Chile. J. S. Am. Earth Sci. 8:33–46.

Hoffman, P. A. 1991. Did the birth of North America turn Gondwana inside out? Science 252:1409–1411.

Ingle, S.; Mueller, P. A.; Heatherington, A. L.; and Kozuch, M. 2003. Isotope evidence for the magmatic and tectonic histories of the Carolina terrane: implications for stratigraphy and terrane affiliation. Tectonophysics 371:187–211.

Jacobshagen, V.; Müller, J.; Wemmer, K.; Ahrendt, A.; and Emmanuil, M. 2002. Hercynian deformation and metamorphism in the Cordillera Oriental of southern Bolivia, central Andes. Tectonophysics 345:119–130.

Keppie, J. D.; Davis, D. W.; and Krogh, T. E. 1998. U-Pb geochronological constraints on the Precambrian stratified units in the Avalon Composite terrane of Nova Scotia, Canada: tectonic implications. Can. J. Earth Sci. 35:222–236.

Keppie, J. D., and Dostal, J. 2007. Rift-related basalt in the 1.2–1.3-Ga granulites of the northern Oaxacan Complex, southern Mexico: evidence for a rifted arc on the northwestern margin of Amazonia. Proc. Geol. Assoc. 118:63–74.

Keppie, J. D., and Ortega-Gutiérrez, F. 1999. Middle America Precambrian basement: a missing piece of the reconstructed 1-Ga orogen. Geol. Soc. Am. Spec. Pap. 336:199–210.

Keppie, J. D., and Ramos, V. 1999. Odyssey of terranes in the Iapetus and Rheic oceans during the Paleozoic. *In* Ramos, V. A., and Keppie, J. D., eds. Laurentia and Gondwana connections before Pangea. Geol. Soc. Am. Spec. Pap. 336:267–276.

Kinny, P. D.; Strachan, R. A.; Kocks, H.; and Friend, C. R. L. 2003. U-Pb geochronology of late Neoproterozoic augen granites in the Moine Supergroup, NW Scotland: dating rift-related, felsic magmatism during supercontinent break-up? J. Geol. Soc. Lond. 160:925–934.

Kontak, D. J.; Clark, A. H.; Farrar, E.; Archibald, D. A.; and Baadsgaard, H. 1990. Late Paleozoic–early Mesozoic magmatism in the Cordillera de Carabaya, Puno, southeastern Peru: geochronology and petrochemistry. J. S. Am. Earth Sci. 3:213–230.

Kontak, D. J.; Clark, A. H.; Farrar, E.; and Strong, D. F. 1985. The rift-associated Permo-Triassic magmatism of the Eastern Cordillera: a precursor of the Andean orogeny. *In* Pitcher, W. S.; Atherton, M. P.; Cobbing, E. J.; and Beckinsale, R. D., eds. Magmatism at a plate edge: the Peruvian Andes. London, Blackie & Son, p. 36–44.

Krogh, T. E. 1973. A low contamination method for decomposition of zircon and extraction of U and Pb for isotopic age determination. Geochim. Cosmochim. Acta 37:485–494.

Litherland, M.; Annells, R. N.; Darbyshire, D. P. F.; Fletcher, C. J. N.; Hawkins, M. P.; Klinck, B. A.; Mitchell, W. I.; et al. 1989. The Proterozoic of eastern Bolivia and its relationship to the Andean mobile belt. Precambrian Res. 43:157–174.

Loewy, S. L.; Connelly, J. N.; and Dalziel, I. W. D. 2004. An orphaned basement block: the Arequipa-Antofalla basement of the central Andean margin of South America. Geol. Soc. Am. Bull. 116:171–187.

Lucassen, F.; Becchio, R.; Wilke, H. G.; Franz, G.; Thirlwall, M. F.; Viramonte, J.; and Wemmer, K. 2000. Proterozoic-Paleozoic development of the basement of the central Andes (18–26°S)—a mobile belt of the South American craton. J. S. Am. Earth Sci. 13:697–715.

Lucassen, F., and Franz, G. 2005. The early Palaeozoic Orogen in the central Andes: a non-collisional orogen comparable to the Cenozoic high plateau? *In* Vaughan, A. R. M.; Leat, P. T.; and Pankhurst, R. J., eds. Terrane processes at the margins of Gondwana. Geol. Soc. Lond. Spec. Publ. 246:257–273.

Lucassen, F.; Trumbull, R.; Franz, G.; Creixell, C.; Vásques, P.; Romer, R. L.; and Figueroa, O. 2004. Distinguishing crustal recycling and juvenile additions at active continental margins: the Paleozoic to recent compositional evolution of the Chilean Pacific margin (36–41°S). J. S. Am. Earth Sci. 17:103–119.

Ludwig, K. J. 2003. Isoplot 3.00. Spec. Publ. 4, Berkeley, CA, Berkeley Geochronology Center, 70 p.

Macfarlane, A. W. 1999. Isotopic studies of northern Andean crustal evolution and ore metal source. *In* Skinner, B. J., ed. Geology and ore deposits in the central Andes. Econ. Geol. Spec. Publ. Ser. 7, p. 195–217.

Macfarlane, A. W.; Tosdal, R. M.; Vidal, C.; and Paredes, J. 1999. Geologic and isotopic constraints on the age and origin of auriferous quartz veins in the Parcoy mining district, Pataz, Perú. *In* Skinner, B., ed., Geology and ore deposits in the central Andes. Econ. Geol. Spec. Publ. Ser. 7, p. 267–279.

Martinez, W.; Valdivia, E.; and Cuyubamba, V. 1998. Geología de los cuadrángulos de Aucayacu, Rio Santa Ana y Tingo María (hojas 18-k, 18-l, 19-k). Boletín Ser. A, Carta Geológica Nacional, vol. 112, Lima, Instituto Geológico Minero y Metalúrgico, 204 p.

McLennan, S. M.; Hemming, S.; McDaniel, D. K.; and Hanson, G. N. 1993. Geochemical approaches to sedimentation, provenance and tectonics. Geol. Soc. Am. Spec. Pap. 284, p.21–40.

Miskovic, A., and Schaltegger, U. 2008. Tectono-magmatic evolution and crustal growth along west-central Amazonia since the late Mesoproterozoic: evidence from the Eastern Cordillera of Peru. 7th International Symposium on Andean Geodynamics (Nice, 2008). Extended abstracts p. 337–338.

Miskovic, A.; Schaltegger, U.; and Chew, D. M. 2005. The Paleozoic-Mesozoic geodynamic transition along

the western Gondwanan margin: geochemical and chronometric constraints from the Eastern Peruvian Cordillera. *In* Abstracts, 3rd Swiss Geoscience Meeting, Zurich.

Murphy, J. B.; Fernandez-Suarez, J.; Jeffries, T.; and Strachan, R. A. 2004*a*. U-Pb (LA-ICP-MS) dating of detrital zircons from Cambrian clastic rocks in Avalonia: erosion of a Neoproterozoic arc along the northern Gondwanan margin. J. Geol. Soc. 161:243–254.

Murphy, J. B.; Pisarevsky, S. A.; Nance, R. D.; and Keppie, D. 2004*b*. Neoproterozoic-Early Paleozoic evolution of peri-Gondwanan terranes: implications for Laurentia-Gondwana connections. Int. J. Earth Sci. 93:659–682.

Murphy, J. B.; Strachan, R.; Nance, R.; Parker, K.; and Fowler, M. 2000. Proto-Avalonia: a 1.2–1.0 Ga tectonothermal event and constraints for the evolution of Rodinia. Geology 28:1071–1074.

Ordóñez-Carmona, O.; Restrepo, J. J.; and Pimentel, M. M. 2006. Geochronological and isotopical review of pre-Devonian crustal basement of the Colombian Andes. J. S. Am. Earth Sci. 21:372–382.

Ortega-Gutierrez, F.; Ruiz, F.; and Centeno-Garcia, E. 1995. Oaxaquia, a Proterozoic microcontinent accreted to North America during the late Paleozoic. Geology 23:1127–1130.

Pankhurst, R., and Rapela, C. W. 1998. The Proto-Andean margin of Gondwana. Geol. Soc. Lond. Spec. Publ. 142, 383 p.

Passchier, C. W., and Trouw, R. A. 1996. Microtectonics. Berlin, Springer, 288 p.

Pitcher, W. S., and Cobbing, E. J. 1985. Phanerozoic plutonism in the Peruvian Andes. In Pitcher, W. S.; Atherton, M. P.; Cobbing, E. J.; and Beckinsale, R. D., eds. Magmatism at a plate edge: the Peruvian Andes. London, Blackie & Son, p. 19–25

Polliand, M.; Schaltegger, U.; Frank, M.; and Fontboté, L. 2005. Formation of intra-arc volcanosedimentary basins in the western flank of the central Peruvian Andes during Late Cretaceous oblique subduction: field evidence and constraints from U-Pb ages and Hf isotopes. Int. J. Earth Sci. 94:231–242.

Quispesivana, L. 1996. Mapa geológico del cuadrángulo de Huanuco, 20K. Lima, Peru, Instituto Geológico Minero y Metalúrgico.

Ramos V. A. 1999. Plate tectonic setting of the Andean Cordillera. Episodes. 22:183–190.

———. 2000. The southern central Andes. *In* Cordani, U. G.; Milani, E. J.; Thomaz-Filho, A.; and Campos, D. A., Tectonic evolution of South America. 31st International Geological Congress, Rio de Janeiro, p. 561–604.

———. 2004. Cuyania, an exotic block to Gondwana: review of a historical success and the present problems. Gondwana Res. 7:1009–1026.

———. 2008*a*. The basement of the central Andes: the Arequipa and related terranes. Ann. Rev. Earth Planet. Sci. 36:289–324.

———. 2008*b*. Patagonia: a Paleozoic continent adrift? J. S. Am. Earth Sci. 26:235–251.

Ramos, V. A., and Aleman, A. 2000. Tectonic evolution of the Andes. *In* Cordani, U. G.; Milani, E. J.; Thomaz-Filho, A.; and Campos, D. A., eds.Tectonic evolution of South America. 31st International Geological Congress, Rio de Janeiro, p. 635–685.

Rapela, C. W.; Pankhurst, R. J.; Casquet, C.; Baldo, E.; Saavedra, J.; Galindo, C.; and Fanning, M. 1998. The Pampean orogeny of the southern proto-Andes: Cambrian continental collision in the Sierras de Cordoba. *In* Pankhurst, R., and Rapela, C. W., eds. The Proto-Andean margin of Gondwana. Geol. Soc. Lond. Spec. Publ. 142:181–218.

Restrepo-Pace, P. 1995. Late Precambrian to Early Mesozoic tectonic evolution of the Colombian Andes, based on new geochronological, geochemical and isotopic data. PhD dissertation, University of Arizona, Tucson. 195 p.

Reusch, D. N.; Van Staal, C. S.; and McNicoll, V. J. 2006. Detrital zircons and Ganderia's southern margin, coastal Maine. Geological Society of America Northeastern Section (39th annual) and Southeastern Section (53rd annual) Joint Meeting, Washington, DC. Session 51, paper 4.

Rogers, N.; Van Staal, C.; McNicoll, V. J.; Pollock, J.; Zagorevski, A.; and Whalen, J. 2006. Neoproterozoic and Cambrian arc magmatism along the eastern margin of the Victoria Lake Supergroup: a remnant of Ganderian basement in central Newfoundland? Precambrian Res. 14:320–341.

Rubatto, D. 2002. Zircon trace element geochemistry: partitioning with garnet and the link between U-Pb ages and metamorphism. Chem. Geol. 184:123–138.

Sato, K.; Tassinari, C.C.G.; Kawashita, K.; and Petronilho, L. 1995. O método geocronológico Sm-Nd no IG/USP e suas aplicações. An. Acad. Bras. Cienc. 67: 313–336.

Sempere, T.; Carlier, G.; Soler, P.; Fornari, M.; Carlotto, V.; Jacay, J.; Arispe, O.; et al. 2002. Late Permian–Middle Jurassic lithospheric thinning in Peru and Bolivia, and its bearing on Andean-age tectonics. Tectonophysics 345:153–181.

Stacey, J. S., and Kramers, J. D. 1975. Approximation of the terrestrial lead isotope evolution by a two-stage model. Earth Planet. Sci. Lett. 26:207–221.

Steiger, R. H., and Jäger, E. 1977. Subcommission on geochronology: convention on the use of decay constants in geo- and cosmochronology. Earth Planet. Sci. Lett. 36:359–362.

Stern, R. A. 1998. High-resolution SIMS determination of radiogenic trace-isotope ratios in minerals. *In* Cabri, L. J., and Vaughan, D. J., eds. Modern approaches to ore and environmental mineralogy. Mineralogical Association of Canada Short Courses, ser. 27, p. 241–268.

Stern, R. J. 2002. Subduction zones. Rev. Geophys., doi: 10.1029/2001RG000108.

Tassinari, C. G.; Bettencourt, J. S.; Geraldes, M. C.; Macambira, M.; and Lafon, J. M. 2000. The Amazonian Craton. *In* Cordani, U. G.; Milani, E. J.; Thomaz, A.; and Campos, D. A. eds. Tectonic evolution of South

America. 31st International Geological Congress, Rio de Janeiro, p. 41–96.

Thomas, W. A., and Astini, R. A. 1996. The Argentine Precordillera: a traveler from the Ouachita embayment of North American Laurentia. Science 273:752–757.

Thomas, W. A.; Astini, R. A.; Mueller, P. A.; Gehrels, G. E.; and Wooden, J. L. 2004. Transfer of the Argentine Precordillera terrane from Laurentia: constraints from detrital-zircon geochronology. Geology 32:965–968.

Tollo, R. P.; Aleinikoff, J. N.; Bartholomew, M. J.; and Rankin, D. W. 2004. Neoproterozoic A-type granitoids of the central and southern Appalachians: intraplate magmatism associated with episodic rifting of the Rodinian supercontinent. Precambrian Res. 128:3–38.

Vabra, G.; Schmid, R.; and Gebauer, D. 1999. Internal morphology, habit and U-Th-Pb microanalysis of amphibolite-to-granulite facies zircons: geochronology of the Ivrea Zone (Southern Alps). Contrib. Mineral. Petrol. 134:380–404.

Van Staal, C. R.; Dewey, J. F.; Mac Niocaill, C.; and Mckerrow, W. S. 1998. The Cambrian-Silurian tectonic evolution of the northern Appalachians and British Caledonide: history of a complex, west and southwest Pacific-type segment of Iapetus. *In* Blundell, D. J., and Scott, A. C., eds. Lyell: the past is the key to the present. Geol. Soc. Lond. Spec. Publ. 143:199–242.

Vinasco, C. J.; Cordani, U. G.; González, H.; Weber, M.; and Pelaez, C. 2006. Geochronological, isotopic, and geochemical data from Permo-Triassic granitic gneisses and granitoids of the Colombian central Andes. J. S. Am. Earth Sci. 21:355–371.

Wasteneys, H. A.; Clark, A. H.; Ferrar, E.; and Langridge, R. J. 1995. Grenvillian granulite-facies metamorphism in the Arequipa Massif, Peru: a Laurentia-Gondwana link. Earth Planet. Sci. Lett. 132:63–73.

Weber, B., and Köhler, H. 1999. Sm-Nd, Rb-S and U-Pb geochronology of a Grenville Terrane in Southern Mexico: origin and geologic history of the Guichicovi Complex. Precambrian Res. 96:245–262.

Williams, I. S. 1998. U-Th-Pb geochronology by ion microprobe. *In* McKibben, M. A.; Shanks, W. C. P., III; and Ridley, W. I., eds. Applications of microanalytical techniques to understanding mineralizing processes. Rev. Econ. Geol. 7:1–35.

Willner, A. P.; Thomson, S. N.; Kröner, A.; Wartho, J.-A.; Wijbrans, J. R.; and Herve, F. 2005. Time markers for the evolution and exhumation history of a Late Palaeozoic paired metamorphic belt in north-central Chile (34°–35°30′S). J. Petrol. 46:1805–1833.

Wilson, J. J., and Reyes, L. 1964. Geologia del cuadrángulo de Pataz. Lima, Carta Geológica Nacional, 91 p.

Zapata, A.; Sánchez, A.; Carrasco, S.; Cardona, A.; Galdos, J. H.; Cerrón F.; and Sempere, T. 2005. The Lower Carboniferous of the western edge of Gondwana in Peru and Bolivia: distribution of sedimentary basins and associated magmatism. 6th International Symposium on Andean Geodynamics (Barcelona, 2005). Extended abstracts, p. 817–820.